Nonlinear Dynamics (2026) 114:569
https://doi.org/10.1007/s11071-026-12422-x

RESEARCH

On a multiple scales perturbation method for partial difference equations

Ege Koroglu[1] · **Wim T. van Horssen**[1]

Received: 15 October 2025 / Revised: 27 January 2026 / Accepted: 25 February 2026

Abstract
In this paper, we introduce a multiple time scales (MTS) framework for partial difference equations (PΔEs). Such a framework is underdeveloped for fully discrete systems. We investigate a classical initial-boundary value problem for a PDE using a standard finite difference discretisation. For a nonlinear example, we additionally apply a nonstandard discretisation. Operators for fast and slow iteration scales are introduced, and secularity conditions governing the slow evolution of modal amplitudes are derived via discrete modal projection. Quantities such as natural frequencies and the stability of periodic solutions are analysed by comparing continuous and discrete MTS approximations. We prove the asymptotic validity of approximations in a Hilbert space setting. For standard discretisations, we derive the bounds on the mode numbers that can be accurately represented by given spatial and temporal resolutions. Beyond these bounds, the discrete natural frequencies can lead to spurious modal interactions, causing the approximations to fail at $\mathcal{O}(\varepsilon)$ accuracy over iteration scales of $\mathcal{O}\left(\frac{1}{\varepsilon}\right)$. For both standard and nonstandard schemes, we obtain qualitatively consistent solutions. Notably, the nonstandard discretisation yields solutions that exactly match the continuous PDE in the limit $\varepsilon = 0$ and closely approximate the continuous MTS expansion for $0 < \varepsilon \ll 1$.

Keywords Multiple scales perturbation methods · Partial difference equations · Nonstandard finite difference method · Initial-boundary value problems · Asymptotics

1 Introduction

Multiple time scales (MTS) methods are well established tools for studying the long time behaviour of weakly nonlinear systems, describing, for instance, wave propagation and nonlinear oscillations. While MTS theory is mature for ordinary differential equations (ODEs), partial differential equations (PDEs) (see e.g. [1–5]) and ordinary difference equations (OΔEs), and recently been extended to differential-delay equations [6], many practical problems in science and engineering require discretisation in both space and time, resulting in partial difference equations (PΔEs). However, the MTS theory for such fully discrete systems remains underdeveloped.

✉ Ege Koroglu
e.koroglu@tudelft.nl

Wim T. van Horssen
w.t.vanhorssen@tudelft.nl

[1] Department of Applied Mathematics, Delft University of Technology, Mekelweg 4, 2628 CD Delft, The Netherlands

The development of MTS theory for OΔEs and recurrence equations goes back to the 1960 s. Torng (1960) [7] and Huston (1970) [8], independently introduced the earliest forms of MTS analysis for OΔEs, both inspired by the Krylov-Bogoliubov method. Despite some differences in notation, their methods are essentially the same: treating weak nonlinearities as forcing terms, solving the linear systems, assuming slowly varying coefficients, applying variation of constants and imposing secularity conditions via Fourier expansions of forcing terms to yield first-order difference equations governing the slow evolution of the amplitudes.

Hoppensteadt and Miranker (1977) [9] were the first to explicitly introduce fast-slow iteration scales, n and $s = \varepsilon n$ with $0 < \varepsilon \ll 1$, for difference equations. They assumed an expansion

$$x_n = x(n, s) = x_0(n, s) + \varepsilon x_1(n, s) + \mathcal{O}(\varepsilon^2),$$

and defined shifted variable as $x_{n+1} = x(n+1, s+\varepsilon)$. Using Taylor expansions like

Published online: 17 April 2026

$$x(n+1, s+\varepsilon) = x(n+1, s) + \varepsilon \tfrac{\partial}{\partial s} x(n+1, s) + \mathcal{O}(\varepsilon^2),$$

they finally obtained secularity conditions in the form of ODEs for the slow variable s, rather than a discrete recurrence relation.

Subramanian (1979) [10] similarly introduced discrete fast and slow time scales with $n_0 = n$ and $n_1 = \epsilon n$. Mimicking the continuous fast-slow time decomposition

$$\frac{\partial}{\partial t} = \frac{\partial}{\partial t_0} + \varepsilon \frac{\partial}{\partial t_1}$$

the discrete difference operator is expanded as

$$\Delta x(n, \varepsilon n) = \Delta_{n_0} x(n, \varepsilon n) + \varepsilon \Delta_{n_1} x(n, \varepsilon n), \tag{1}$$

where $\Delta_{n_0} x(n, \varepsilon n) = x(n+1, \varepsilon n) - x(n, \varepsilon n)$ and $\Delta_{n_1} x(n, \varepsilon n) = x(n, \varepsilon n + \varepsilon) - x(n, \varepsilon n)$. In contrast to Hoppensteadt and Miranker, this method leads to discrete secularity conditions that directly determine the slowly varying modal amplitudes.

Van Horssen and ter Brake (2009) [11] further developed the method for OΔEs, also obtaining discrete secularity conditions similar to those in Subramanian's approach. Their main innovation lies in a more rigorous treatment of the discrete operators. Rather than mimicking the continuous analogue, they derived the difference operators from fundamental definitions:

$$\begin{aligned} \Delta &= E_n - I \\ &= E_{n_0} E_{n_1} - I \\ &= \Delta_{n_0} + \Delta_{n_1} + \Delta_{n_0} \Delta_{n_1} \end{aligned} \tag{2}$$

where

$$\begin{aligned} E_n x(n, \varepsilon n) &= x(n+1, \varepsilon n + \varepsilon), \\ E_{n_0} x(n, \varepsilon n) &= x(n+1, \varepsilon n), \\ E_{n_1} x(n, \varepsilon n) &= x(n, \varepsilon n + \varepsilon) \end{aligned} \tag{3}$$

with $\Delta_{n_0} = \mathcal{O}(1)$ and $\Delta_{n_1} = \mathcal{O}(\varepsilon)$. They pointed out that the expansion used by Subramanian overlooks the mixed difference term $\Delta_{n_0} \Delta_{n_1}$, which contributes to the secularity condition. This omission is a crucial flaw of that approach. Furthermore, Van Horssen and ter Brake emphasized that because the behaviour of OΔEs and their corresponding ODEs may differ substantially, applying continuous-type secularity conditions as in Hoppensteadt and Miranker's method can yield approximations that are not $\mathcal{O}(\varepsilon)$ accurate over $\mathcal{O}(\frac{1}{\varepsilon})$ iteration scales.

Following the criticisms of van Horssen and ter Brake [11] on the method of Hoppensteadt and Miranker [9], Hall and Lustri (2016) [12] demonstrated that combining MTS with a continuous slow time scale and matched asymptotic expansions can still capture the key characteristics of the problem.

Liu (2018) [13] introduced an alternative analytical framework for difference equations using renormalisation. The method uses Newton–Maclaurin expansions to obtain uniformly valid asymptotic approximations and reduced slow dynamics without explicit multiple time scales.

Compared to OΔEs, the literature on MTS for partial difference equations is even more limited. Newell (1977) [14] studied explicit initial-value partial difference schemes, aiming to determine nonlinear stability near linear stability bounds. He used an asymptotic expansion assuming slow variation in spatial and temporal indices, rather than formally separating fast and slow time scales. This approach therefore does not align with the formal MTS framework. More recently, Hyatt and colleagues (2025) [15] applied a semi-discretisation in time to the Korteweg-de Vries (KdV) equation, using a Hoppensteadt and Miranker-like approach to derive slow modulation equations for the resulting system with travelling wave solutions.

The method proposed in [9] has become the most widely used framework for applying MTS to difference equations. Some notable examples of subsequent works applying or extending this approach to OΔEs include [16–18].

Nonstandard finite difference (NSFD) schemes were introduced by Mickens [19] to better preserve qualitative features of the underlying continuous models in discrete formulations. These methods have since been extensively developed for both OΔEs and PΔEs. Several studies have specifically applied NSFD schemes to initial boundary value problems (IBVPs) for PΔEs, including [20–24].

As reflected in the disproportion between the literature on OΔEs and PΔEs, further development is needed for PΔEs. In this paper, we extend the theory of MTS perturbation methods from OΔEs to PΔEs. To demonstrate the resulting framework, we apply it to a nonlinear initial boundary value problem (IBVP) discretised using both standard and nonstandard finite difference schemes.

In this paper, a multiple time scales (MTS) framework for PΔEs, obtained by the spatial and temporal discretisation of partial differential equations, is developed. To establish this framework, partial difference operators incorporating fast and slow iteration scales are introduced. Following this, to illustrate the approach clearly, a linear PDE is discretised using finite differences, and the resulting MTS approximation is compared with both the continuous PDEs MTS approximation and its exact solution. The asymptotic validity of the MTS approximations are established in a Hilbert space setting. Finally, the method is applied to a nonlinear PΔE derived from a string-like PDE with a Rayleigh-type of nonlinearity, discretised using both standard and nonstandard finite difference schemes. The resulting discrete approxima-

tions are then compared to the corresponding continuous PDE approximations.

The main contributions of this study include:

- Extending MTS analysis to initial boundary value problem for PΔEs.
- Deriving a nonstandard difference scheme that is exact for $\varepsilon = 0$ and is equivalent to the MTS approximation of the PDE for $0 < \varepsilon \ll 1$.
- Proving the asymptotic validity of the MTS approximation of the PΔE.
- Comparing the modal equilibria of the continuous PDE problem with the MTS approximations of the PΔE problem.

The structure of this study is as follows: Sect. 2 provides preliminaries on partial difference equations in the context of multiple scales. Following the preliminaries, a linear PDE is analysed, and both its exact solution and MTS approximation are derived. The corresponding PΔE is discretised, its MTS approximation is obtained, and the results are compared with the continuous analogue and the exact solution. Section 3 then establishes the asymptotic validity of these MTS approximations within an infinite-dimensional Hilbert space framework. Section 4 investigates a weakly nonlinear PDE, applying the MTS approximation both to the continuous problem and to its standard and nonstandard discrete formulations. Finally, Sect. 5 concludes with a discussion of the results, limitations, and prospects for future work.

2 Setup of the method

2.1 Discrete operators and time scales

Operators

We define the discrete operators that form the basis of multiple scales perturbation methods for both ordinary and partial difference equations.

We begin with the three primary difference operators: the identity operator I, the shift operator E and the difference operator Δ, defined for a scalar function $x(n)$ as:

$$\begin{aligned} Ix(n) &:= x(n), \\ Ex(n) &:= x(n+1), \\ \Delta x(n) &:= x(n+1) - x(n). \end{aligned} \tag{4}$$

Following from the definition of the shift operator, we introduce the inverse shift operator E^{-1}, which satisfies $EE^{-1} = E^{-1}E = I$. It can be written explicitly as

$$E^{-1}x(n) := x(n-1). \tag{5}$$

We can briefly write

$$\Delta = E - I. \tag{6}$$

To study partial difference equations, we extend these definitions to a multivariate setting. Restricting ourselves to two discrete variables, we define for $x = x(i,n)$:

$$\begin{aligned} E_i x(i,n) &= x(i+1,n), \\ E_i^{-1} x(i,n) &= x(i-1,n), \\ \Delta_i x(i,n) &= (E_i - I)x(i,n), \\ E_n x(i,n) &= x(i,n+1), \\ E_n^{-1} x(i,n) &= x(i,n-1), \\ \Delta_n x(i,n) &= (E_n - I)x(i,n). \end{aligned} \tag{7}$$

We now assume that the variable n carries dynamics on both a fast scale and a slow scale:

$$n_0 = n_0(n) := n, \quad n_1 = n_1(n) := \varepsilon n, \tag{8}$$

so that the sequence $x(i,n)$ becomes a function of both scales: $x(i,n) \to x(i,n_0,n_1) = x(i,n,\varepsilon n)$. The given form of two-scale extension was first introduced in [11] for $O\Delta Es$. Following the fast and slow scales (8), and definitions in (6)-(7), the extended operators acting on $x(i,n,\varepsilon n)$ are given by:

$$\begin{aligned} E_i x(i,n,\varepsilon n) &= x(i+1,n,\varepsilon n), \\ \Delta_i x(i,n,\varepsilon n) &= (E_i - I)x(i,n,\varepsilon n), \\ E_{n_0} x(i,n,\varepsilon n) &= x(i,n+1,\varepsilon n), \\ \Delta_{n_0} x(i,n,\varepsilon n) &= (E_{n_0} - I)x(i,n,\varepsilon n), \\ E_{n_1} x(i,n,\varepsilon n) &= x(i,n,\varepsilon n + \varepsilon), \\ \Delta_{n_1} x(i,n,\varepsilon n) &= (E_{n_1} - I)x(i,n,\varepsilon n). \end{aligned} \tag{9}$$

The corresponding inverse shift operators in space and time follow directly from these definitions.

The full time shift operator E_n is then composed of the fast and slow shifts:

$$\begin{aligned} E_n x(i,n_0,n_1) &= E_n x(i,n,\varepsilon n) \\ &= x(i,n+1,\varepsilon n + \varepsilon) \\ &= E_{n_0} E_{n_1} x(i,n_0,n_1). \end{aligned} \tag{10}$$

Using this composition and (6), the total time (or iteration)-difference operator becomes:

$$\begin{aligned} \Delta_n &= E_n - I \\ &= E_{n_0} E_{n_1} - I \\ &= \Delta_{n_0} + \Delta_{n_1} + \Delta_{n_0}\Delta_{n_1}. \end{aligned} \tag{11}$$

Based on Taylor expansions (see [11]), we note the orders of the fast and slow difference operators:

$$\begin{aligned}\Delta_i x(i,n,\varepsilon n) =&\mathcal{O}(x(i,n,\varepsilon n)),\\ \Delta_{n_0} x(i,n,\varepsilon n) =&\mathcal{O}(x(i,n,\varepsilon n)),\\ \Delta_{n_1} x(i,n,\varepsilon n) =&\mathcal{O}(\varepsilon x(i,n,\varepsilon n)).\end{aligned} \tag{12}$$

It is convenient to use difference operators rather than shift operators because they directly indicate the orders of magnitude of terms in the equations. Thus, we adopt this choice in the difference stencils obtained from discretisations.

Inner product

Where the time and space discretisation step sizes are uniform and are given by Δt and Δx, respectively, we use the discrete analogue of the L^2 inner product on a uniform spatial grid $x_i = i\Delta x$, where $x_i \in \{0, \Delta x, \ldots, 1-\Delta x, 1\}$, as

$$\langle f, g\rangle := \Delta x \sum_{i=0}^{1/\Delta x} f(i)g(i). \tag{13}$$

2.2 Analytical example and its MTS solution

In this subsection we consider the following damped wave equation on the unit interval:

$$u_{tt} - u_{xx} + \varepsilon u_t = 0, \tag{14}$$

where $x \in (0,1)$ and $t > 0$ with homogeneous boundary conditions $u(0,t) = u(1,t) = 0$ and given initial conditions $u(x,0) = f(x)$ and $u_t(x,0) = g(x)$.

We define the modal coefficients associated with the initial conditions as

$$\begin{aligned}A_k :=& 2\int_0^1 f(x)\sin(k\pi x)dx,\\ B_k :=& \tfrac{2}{\omega_k(\varepsilon)}\int_0^1 g(x)\sin(k\pi x)\,dx,\end{aligned} \tag{15}$$

where damped natural frequencies are given by

$$\omega_k(\varepsilon) := \sqrt{k^2\pi^2 - \frac{\varepsilon^2}{4}}. \tag{16}$$

Throughout this example we restrict to the underdamped case. In particular, we assume $0 < \varepsilon \le 2\pi$, so that $\omega_k(\varepsilon)$ is real for every $k \in \mathbb{N}$. Using the method of separation of variables, the eigenfunctions satisfying the homogeneous Dirichlet boundary conditions are $\varphi_k(x) = \sin(k\pi x)$ (so $\varphi_k(0) = \varphi_k(1) = 0$ for all $k \in \mathbb{N}$). Hence, the exact solution of Eq. (14) can be written as

$$\begin{aligned}u(x,t) = \sum_{k=1}^{\infty} e^{-\frac{\varepsilon t}{2}}\Big(&A_k\cos(\omega_k(\varepsilon)t)\\ &+B_k\sin(\omega_k(\varepsilon)t)\Big)\sin(k\pi x).\end{aligned} \tag{17}$$

We now further consider weakly-damped case $0 < \varepsilon \ll 1$ and construct a multiple time scales approximation by introducing the expansion

$$u(x,t) = u_0(x,t_0,t_1) + \varepsilon u_1(x,t_0,t_1) + \mathcal{O}(\varepsilon^2),$$

where the fast and and slow times are $t_0 = t, t_1 = \varepsilon t$, respectively. This leads to the leading order problems

$$\begin{aligned}\mathcal{O}(1): &\quad \partial_{t_0}^2 u_0 - \partial_x^2 u_0 = 0\\ \mathcal{O}(\varepsilon): &\quad \partial_{t_0}^2 u_1 - \partial_x^2 u_1 = -2\partial_{t_0}\partial_{t_1}u_0 - \partial_{t_0}u_0,\end{aligned}$$

with u_0 and u_1 satisfying homogeneous Dirichlet boundary conditions at $x = 0, 1$. At leading order, the approximation is given by

$$\begin{aligned}u_0(x,t_0,t_1) = \sum_{k=1}^{\infty}\Big(&A_k(t_1)\cos(k\pi t_0)\\ &+B_k(t_1)\sin(k\pi t_0)\Big)\sin(k\pi x)\end{aligned} \tag{18}$$

where the modal amplitudes evolve according to

$$A_k(t_1) = e^{-\frac{t_1}{2}}A_k(0), \quad B_k(t_1) = e^{-\frac{t_1}{2}}B_k(0). \tag{19}$$

2.3 Discretised problem and its MTS approximation

Having derived the exact solution (17) and the multiple timescales (MTS) approximation (18) of the continuous problem (14), we now study its discretised counterpart. Our goal is to construct the corresponding MTS expansion for the discrete scheme and compare its structure to that of the continuous case.

We discretise the PDE (14) using a standard second-order central differences. Let $U(i,n)$ denote the discrete approximation of $u(x,t)$, defined on uniform spatial and temporal grids, defined as $x_i = i\Delta x$, for $i = 0, 1, \ldots, M = \frac{1}{\Delta x}$, and $t_n = n\Delta t$ for $n \in \mathbb{N}$. Applying central differences for each term in (14), yields to the following explicit finite difference scheme:

$$\begin{aligned}&\frac{U(i,n+1) - 2U(i,n) + U(i,n-1)}{(\Delta t)^2}\\ &- \frac{U(i+1,n) - 2U(i,n) + U(i-1,n)}{(\Delta x)^2}\\ &+\varepsilon\frac{U(i,n+1) - U(i,n-1)}{2\Delta t} = 0.\end{aligned} \tag{20}$$

Using the operators defined in (7), Eq. (20) can be written compactly as $LU(i,n) = 0$ with

$$L := \frac{\Delta_n^2 E_n^{-1}}{(\Delta t)^2} - \frac{\Delta_i^2 E_i^{-1}}{(\Delta x)^2} + \varepsilon \frac{(\Delta_n^2 + 2\Delta_n)E_n^{-1}}{2\Delta t}. \tag{21}$$

It is convenient, however, to use the equivalent time-shifted partial difference operator, which simplifies the separation of time-scales in asymptotic expansions:

$$L := \frac{\Delta_n^2}{(\Delta t)^2} - \frac{\Delta_i^2 E_i^{-1} E_n}{(\Delta x)^2} + \varepsilon \frac{\Delta_n^2 + 2\Delta_n}{2\Delta t}. \tag{22}$$

Hence, we adopt this forward time-shifted operator for the discretised PDE.

A naïve perturbation expansion applied to Eq. (22) leads to secular terms in the discrete solution. To avoid this, we introduce a two time-scales expansion of the form:

$$U(i,n) = U_0(i,n_0,n_1) + \varepsilon U_1(i,n_0,n_1) + \mathcal{O}(\varepsilon^2), \tag{23}$$

where the fast and slow iteration scales are defined as $n_0 = n_0(n) := n$ and $n_1 = n_1(n) := \varepsilon n$, respectively.

From the expansion of the time-difference operator (cf. Equation (12)), we know that

$$\Delta_n^2 = \Delta_{n_0}^2 + 2\Delta_{n_1}\Delta_{n_0}(\Delta_{n_0} + I) + \mathcal{O}(\varepsilon^2).$$

Substituting the two time-scales expansion into Eq. (22) yields:

$$\begin{aligned} LU = 0 \rightarrow & (L_0 + L_1 + \mathcal{O}(\varepsilon^2))(U_0 + \varepsilon U_1 + \mathcal{O}(\varepsilon^2)) \\ & = L_0 U_0 + \varepsilon L_0 U_1 + L_1 U_0 + \mathcal{O}(\varepsilon^2) = 0, \end{aligned} \tag{24}$$

where the operators L_0 and L_1 are given by

$$L_0 := \frac{\Delta_{n_0}^2}{(\Delta t)^2} - \frac{\Delta_i^2 E_i^{-1} E_{n_0}}{(\Delta x)^2}, \tag{25a}$$

$$L_1 := \frac{2\Delta_{n_1}(\Delta_{n_0}^2 + \Delta_{n_0})}{(\Delta t)^2} - \frac{\Delta_i^2 \Delta_{n_1} E_{n_0}}{(\Delta x)^2} + \varepsilon \frac{\Delta_{n_0}^2 + 2\Delta_{n_0}}{2\Delta t}. \tag{25b}$$

Recalling from (12) that $\Delta_{n_1} = \mathcal{O}(\varepsilon)$, it follows that $L_1 U_0 = \mathcal{O}(\varepsilon)$. Hence, the leading order problems become:

$$\mathcal{O}(1): \quad L_0 U_0 = 0, \tag{26a}$$

$$\mathcal{O}(\varepsilon): \quad \varepsilon L_0 U_1 = -L_1 U_0. \tag{26b}$$

To solve Eq. (26a), we use the method of separation of variables by setting

$$U_0(i,n_0,n_1) = V_0(n_0,n_1)\,\varphi(i),$$

which leads to

$$\frac{[\Delta_{n_0}^2 V_0(n_0,n_1)]\varphi(i)}{(\Delta t)^2} - \frac{[\Delta_i^2 E_i^{-1}\varphi(i)][E_{n_0} V_0(n_0,n_1)]}{(\Delta x)^2} = 0. \tag{27}$$

Dividing both sides by the common factors $E_{n_0} V_0(n_0,n_1)\,\varphi(i)$, and introducing a separation constant λ, we obtain

$$\frac{\Delta_{n_0}^2 V_0(n_0,n_1)}{(\Delta t)^2 E_{n_0} V_0(n_0,n_1)} = \frac{\Delta_i^2 E_i^{-1}\varphi(i)}{(\Delta x)^2 \varphi(i)} = -\lambda. \tag{28}$$

The spatial problem then becomes

$$\varphi(i+1) + (\lambda(\Delta x)^2 - 2)\varphi(i) + \varphi(i-1) = 0. \tag{29}$$

The characteristic roots of this equation are

$$r_{1,2} = 1 - \frac{\lambda(\Delta x)^2}{2} \pm i\sqrt{\lambda(\Delta x)^2 - \frac{\lambda^2(\Delta x)^4}{4}}. \tag{30}$$

Imposing $\varphi(0) = \varphi(M) = 0$ yields discrete eigenpairs

$$\varphi_k(i) = \sin(k\pi i \Delta x), \tag{31a}$$

$$\lambda_k = \frac{4}{(\Delta x)^2}\sin^2\left(\frac{k\pi\Delta x}{2}\right), \tag{31b}$$

with $k \in \mathbb{N}^+$, $M\Delta x = 1$, and $i = 0, 1, \ldots, M = \frac{1}{\Delta x}$. These satisfy $\lambda_k < \frac{4}{(\Delta x)^2}$, hence the square-root term in (30) is real and $|r_{1,2}| = 1$. Further details on the derivation of the eigenvalues in (31b) are provided in § 4.2. Using this separation constant λ_k, one can similarly obtain the temporal equation as

$$V_0(n+2,\cdot) + (\lambda_k(\Delta t)^2 - 2)V_0(n+1,\cdot) + V_0(n,\cdot) = 0, \tag{32}$$

which has characteristic roots

$$r_{1,2} = 1 - \frac{\lambda_k(\Delta t)^2}{2} \pm i\sqrt{\lambda_k(\Delta t)^2 - \frac{\lambda_k^2(\Delta t)^4}{4}}. \tag{33}$$

Imposing $\lambda_k < \frac{4}{(\Delta t)^2}$ ensures $|r_{1,2}| = 1$, yielding oscilla-

tory solutions without spurious damping or amplification and keeping the discrete dynamics consistent with the intended continuous model. This yields the general solution

$$\begin{aligned} V_{0k}(n_0, n_1) =& A_k(n_1)\cos(\widetilde{\omega_k} n_0 \Delta t) \\ &+ B_k(n_1)\sin(\widetilde{\omega_k} n_0 \Delta t), \end{aligned} \tag{34}$$

where the frequency $\widetilde{\omega_k}$ satisfies

$$\begin{aligned} \cos(\widetilde{\omega_k}\Delta t) =& 1 - \frac{\lambda_k(\Delta t)^2}{2}, \\ \sin(\widetilde{\omega_k}\Delta t) =& \sqrt{\lambda_k(\Delta t)^2 - \frac{\lambda_k^2(\Delta t)^4}{4}}. \end{aligned} \tag{35}$$

Hence, we can write

$$\begin{aligned} \widetilde{\omega_k} = \tfrac{1}{\Delta t}\arcsin\Bigg[& \left(1 + \tfrac{4}{(\Delta x)^2}\sin^2\left(\tfrac{\pi k \Delta x}{2}\right)\right)(\Delta t)^2 \\ & - \left(1 + \tfrac{4}{(\Delta x)^2}\sin^2\left(\tfrac{\pi k \Delta x}{2}\right)\right)^2 \tfrac{(\Delta t)^4}{4}\Bigg]^{\frac{1}{2}}. \end{aligned} \tag{36}$$

This results in the solution of the $\mathcal{O}(1)$ problem

$$\begin{aligned} U_0(i, n_0, n_1) = \sum_{k=1}^{\infty} \big[& A_k(n_1)\cos(\widetilde{\omega_k}\Delta t n_0) \\ & + B_k(n_1)\sin(\widetilde{\omega_k}\Delta t n_0)\big]\sin(k\pi i \Delta x). \end{aligned} \tag{37}$$

Substituting this into Eq. (26b) and taking the inner product (as defined in Eq. (13)) with φ_m as defined in (31a), we obtain

$$\varepsilon\langle L_0 U_1, \varphi_m\rangle = -\langle L_1 U_0, \varphi_m\rangle. \tag{38}$$

Assuming

$$U_1(i, n_0, n_1) = \sum_{k=1}^{\infty} V_{1k}(n_0, n_1)\varphi_k(i), \tag{39}$$

Equation (38) becomes

$$\varepsilon\langle L_0 \sum_{k=1}^{\infty} V_{1k}\varphi_k, \varphi_m\rangle = -\langle L_1 \sum_{k=1}^{\infty} V_{0k}\varphi_k, \varphi_m\rangle. \tag{40}$$

Using linearity and orthogonality, we get for each $m \in \mathbb{N}$:

$$\begin{aligned} & -\varepsilon\left(\frac{\Delta_{n_0}^2}{(\Delta t)^2}V_{1m} + \lambda_m E_{n_0} V_{1m}\right) \\ =& \Delta_{n_1}\frac{\Delta_{n_0}^2 + 2\Delta_{n_0}}{(\Delta t)^2}V_{0m} + \varepsilon\frac{\Delta_{n_0}^2 + 2\Delta_{n_0}}{2\Delta t}V_{0m}. \end{aligned} \tag{41}$$

Since the kernel of left-hand side of Eq. (41) is spanned by $\sin(\omega_m \Delta t\, n_0)$ and $\cos(\omega_m \Delta t\, n_0)$, and to avoid the secular growth of the leading order solution (37), we let $A_m(n_1)$ and $B_m(n_1)$ be such that the right-hand side of Eq. (41) does not project onto this kernel.

To determine the required conditions, we expand

$$\begin{aligned} & (\Delta_{n_0}^2 + 2\Delta_{n_0})V_{0m} \\ =& \cos(\widetilde{\omega_m} n \Delta t) \\ & \times \underbrace{[A_m\cos(2\widetilde{\omega_m}\Delta t) + B_m\sin(2\widetilde{\omega_m}\Delta t) - A_m]}_{=:F_m} \\ & + \sin(\widetilde{\omega_m} n \Delta t) \\ & \times \underbrace{[-A_m sin(2\widetilde{\omega_m}\Delta t) + B_m\cos(2\widetilde{\omega_m}\Delta t) - B_m]}_{=:G_m} \\ =& F_m\cos(\widetilde{\omega_m} n \Delta t) + G_m\sin(\widetilde{\omega_m} n \Delta t). \end{aligned} \tag{42}$$

Substituting this into the right-hand side of (41), secular terms are eliminated by requiring

$$\Delta_{n_1} F_m = -\varepsilon\frac{\Delta t}{2}F_m, \quad \Delta_{n_1} G_m = -\varepsilon\frac{\Delta t}{2}G_m. \tag{43}$$

Equivalently, in terms of slow time steps:

$$\begin{aligned} F_m(\varepsilon n + \varepsilon) &= \left(1 - \varepsilon\frac{\Delta t}{2}\right)F_m(\varepsilon n), \\ G_m(\varepsilon n + \varepsilon) &= \left(1 - \varepsilon\frac{\Delta t}{2}\right)G_m(\varepsilon n). \end{aligned} \tag{44}$$

This yields exponential decay for iteration steps $n \lesssim \frac{1}{\varepsilon}$:

$$\begin{aligned} F_m(\varepsilon n) &= \left(1 - \varepsilon\frac{\Delta t}{2}\right)^n F_m(0) \simeq e^{-\frac{\varepsilon n \Delta t}{2}}F_m(0), \\ G_m(\varepsilon n) &\simeq e^{-\frac{\varepsilon n \Delta t}{2}}G_m(0). \end{aligned} \tag{45}$$

We have obtained the identical eigenfunctions for the discretised system ($\varphi_k = \sin(k\pi i \Delta x)$) as in the exact PDE solution and the MTS approximation of this PDE ($\varphi_k = \sin(k\pi x)$). However, the discretisation has an influence on the corresponding eigenvalues, λ_k, hence on the natural frequencies $\widetilde{\omega_k}$.

From (18) and (16), we observe that the MTS approximations for the continuous PDE have frequencies $\omega_k = k\pi$, which are accurate up to $\mathcal{O}(\varepsilon^2)$ compared to the exact damped frequencies of the PDE. The decay factor in both the exact solution (17) and the MTS approximation (19) are identical, given by $e^{\frac{-\varepsilon t}{2}}$.

In contrast, from (35) and (31b), the natural frequency of the discrete system (36) $\widetilde{\omega_k}$ does not equal the continuous PDEs frequency or its MTS approximation. The discrete frequency depends explicitly on the spatial and temporal grid

resolutions Δx and Δt. We will examine how closely these discrete frequencies approximate the continuous MTS frequencies in later chapters.

For small ε, and recognizing that $\Delta t\, n = t_n$, the discrete decay factors of F_m and G_m in (45) tend to $e^{\frac{-\varepsilon t_n}{2}}$. The relationship between the modal amplitudes A_m, B_m and F_m, G_m given in (42), shows that while they share the same rate of decay to leading order in ε, the actual modal amplitudes do not match exactly due to discretisation effects. Furthermore, notice from their definitions (42) that for larger mode numbers m, the F_m and G_m deviates from A_m and B_m. Hence, despite differences in frequency content and amplitudes, the MTS approximations for continuous PDE and its discretisation exhibit consistent leading-order damping behaviour.

Overall, even in the limit $\varepsilon = 0$, the discrete system does not exactly reproduce the continuous PDE frequency or amplitude contents due to the dependence on spatial and temporal grid resolutions. In this linear example, there is no time dependence or nonlinearities. Therefore, phenomena such as modal interactions do not arise in this case. These interactions make the analysis more interesting, as discretisation can qualitatively alter the system's behaviour. In § 4, we examine a nonlinear system where modal interactions arise and explore how discretisation affects them.

3 Asymptotic validity

The first rigorous construction of the asymptotic validity of the multiple time scales perturbation approximation for difference equations was provided by van Horssen and Ter Brake in [11].

In the present section, we extend the theory to partial difference equations (PΔE), or equivalently, to infinite-dimensional difference systems. This extension requires the formulation of the suitable Hilbert space framework that accommodates the modal decomposition arising from the spatial discretisation of partial differential equations.

Therefore, we first introduce the necessary function spaces used in our analysis.

Definition 1 (Hilbert Space Framework) Let each mode k be represented by a vector $\boldsymbol{w}_k(n) \in \mathbb{R}^d$ at iteration step $n \in \mathbb{N}$. The dimension $d \in \mathbb{N}$ corresponds to the order of the system (e.g., $d = 2$ for second order in time). We define the state vector as

$$\begin{aligned} \boldsymbol{W}(n) :=& (\boldsymbol{w}_1(n), \boldsymbol{w}_2(n), \dots) \\ =& \bigoplus_{k=1}^{\infty} \boldsymbol{w}_k(n), \quad \boldsymbol{w}_k(n) \in \mathbb{R}^d, \end{aligned} \tag{46}$$

and the associated Hilbert space as

$$\mathcal{H} := \ell^2(\mathbb{N}; \mathbb{R}^d) = \left\{ \boldsymbol{W} \,\middle|\, \sum_{k=1}^{\infty} \|\boldsymbol{w}_k\|^2 < \infty \right\}. \tag{47}$$

We define a linear operator $\mathcal{A} : \mathcal{H} \to \mathcal{H}$ by

$$\mathcal{A} := \bigoplus_{k=1}^{\infty} A_k, \tag{48}$$

with $A_k \in \mathbb{R}^{d\times d}$, assumed to be diagonalisable as $A_k = P_k \Lambda_k P_k^{-1}$, where $\Lambda_k = \operatorname{diag}(\lambda_k^{(1)}, \dots, \lambda_k^{(d)})$. This direct sum construction yields a block-diagonal structure, acting component-wise:

$$\mathcal{A}(\boldsymbol{W}) = (A_1 \boldsymbol{w}_1, A_2 \boldsymbol{w}_2, \dots). \tag{49}$$

We similarly define the block operators $\mathcal{P}, \mathcal{L} : \mathcal{H} \to \mathcal{H}$ by

$$\mathcal{P} := \bigoplus_{k=1}^{\infty} P_k, \quad \mathcal{L} := \bigoplus_{k=1}^{\infty} \Lambda_k. \tag{50}$$

We assume that the block operators $\mathcal{P}$, $\mathcal{P}^{-1}$, and $\mathcal{L}$ are bounded on $\mathcal{H}$ with norms satisfying

$$\kappa := \|\mathcal{P}\| \left\|\mathcal{P}^{-1}\right\| < \infty, \quad \lambda := \|\mathcal{L}\| < \infty. \tag{51}$$

The nonlinear operator $\boldsymbol{F} : \mathcal{H} \to \mathcal{H}$ is defined component-wise as

$$\boldsymbol{F}(\boldsymbol{W}) := \bigoplus_{k=1}^{\infty} \boldsymbol{f}_k(\boldsymbol{W}), \quad \boldsymbol{f}_k : \mathcal{H} \to \mathbb{R}^d. \tag{52}$$

We assume that $\boldsymbol{F}$ is Lipschitz continuous:

$$\left\|\boldsymbol{f}_k(\boldsymbol{W}_1) - \boldsymbol{f}_k(\boldsymbol{W}_2)\right\|_{\mathbb{R}^d} \le L_k \|\boldsymbol{W}_1 - \boldsymbol{W}_2\|_{\mathcal{H}}, \tag{53}$$

with $L = (\sum_{k=1}^{\infty} L_k^2)^{1/2}$. This implies

$$\begin{aligned} \|\boldsymbol{F}(\boldsymbol{W}_1) - \boldsymbol{F}(\boldsymbol{W}_1)\|_{\mathcal{H}}^2 &= \sum_{k=1}^{\infty} \left\|\boldsymbol{f}_k(\boldsymbol{W}_1) - \boldsymbol{f}_k(\boldsymbol{W}_2)\right\|_{\mathbb{R}^d} \\ &\le \sum_{k=1}^{\infty} L_k^2 \|\boldsymbol{W}_1 - \boldsymbol{W}_2\|_{\mathcal{H}}^2 \\ &= \|\boldsymbol{W}_1 - \boldsymbol{W}_2\|_{\mathcal{H}}^2 \sum_{k=1}^{\infty} L_k^2 \\ &= L^2 \|\boldsymbol{W}_1 - \boldsymbol{W}_2\|_{\mathcal{H}}^2. \end{aligned} \tag{54}$$

Theorem 1 (Asymptotic Validity) *Let the state vector $\boldsymbol{W}(n)$ evolve according to the discrete system*

$$\boldsymbol{W}(n+1) = \mathcal{A}\boldsymbol{W}(n) + \varepsilon \boldsymbol{F}(\boldsymbol{W}(n)), \tag{55}$$

and let $\widetilde{\boldsymbol{W}}(n)$ be its multiple time scales approximation satisfying

$$\widetilde{\boldsymbol{W}}(n+1) = \mathcal{A}\widetilde{\boldsymbol{W}}(n) + \varepsilon \boldsymbol{F}(\widetilde{\boldsymbol{W}}(n)) + \varepsilon^{m+1}\boldsymbol{R}(n), \tag{56}$$

where $\boldsymbol{R}(n) \in \mathcal{H}$ is the residual term. With λ defined in (51), the following holds:

$$\left\| \widetilde{\boldsymbol{W}}(0) - \boldsymbol{W}(0) \right\|_{\mathcal{H}} = \mathcal{O}(\varepsilon^m),$$

then for $n = \mathcal{O}(\frac{1}{\varepsilon})$ and any $\lambda > 0$,

$$\left\| \widetilde{\boldsymbol{W}}(n) - \boldsymbol{W}(n) \right\|_{\mathcal{H}} = \mathcal{O}(\varepsilon^m \lambda^n).$$

Proof We investigate each scenario for λ, i.e., $0 < \lambda < 1$, $\lambda = 1$ and $\lambda > 1$.

We begin with $0 < \lambda \leq 1$. We introduce the transformed variables $\boldsymbol{U}(n) := P^{-1}\boldsymbol{W}(n)$, which leads to:

$$\begin{aligned} \boldsymbol{U}(n+1) &= \Lambda \boldsymbol{U}(n) + \varepsilon P^{-1}\boldsymbol{F}(P\boldsymbol{U}(n)), \\ \widetilde{\boldsymbol{U}}(n+1) &= \Lambda \widetilde{\boldsymbol{U}}(n) + \varepsilon P^{-1}\boldsymbol{F}(P\widetilde{\boldsymbol{U}}(n)) + \varepsilon^{m+1} P^{-1}\boldsymbol{R}(n). \end{aligned} \tag{57}$$

Subtracting these, and applying the $\mathcal{H}$-norm yields

$$\begin{aligned} &\left\| \widetilde{\boldsymbol{U}}(n+1) - \boldsymbol{U}(n+1) \right\|_{\mathcal{H}} \\ &\leq \|\Lambda\| \left\| \widetilde{\boldsymbol{U}}(n) - \boldsymbol{U}(n) \right\|_{\mathcal{H}} \\ &+ \varepsilon \left\| P^{-1} \right\| \left\| \boldsymbol{F}(P\widetilde{\boldsymbol{U}}(n)) - \boldsymbol{F}(P\boldsymbol{U}(n)) \right\|_{\mathcal{H}} \\ &+ \varepsilon^{m+1} \left\| P^{-1} \right\| \|\boldsymbol{R}(n)\|_{\mathcal{H}}. \end{aligned} \tag{58}$$

Using Lipschitz continuity of $\boldsymbol{F}$, we estimate

$$\left\| \boldsymbol{F}(P\widetilde{\boldsymbol{U}}(n)) - \boldsymbol{F}(P\boldsymbol{U}(n)) \right\|_{\mathcal{H}} \leq L \|P\| \left\| \widetilde{\boldsymbol{U}}(n) - \boldsymbol{U}(n) \right\|_{\mathcal{H}}. \tag{59}$$

Using from (51) that $\kappa = \|P\| \left\| P^{-1} \right\|$, and assuming that there exists a constant $\widetilde{C}$ such that $\left\| P^{-1} \right\| \|\boldsymbol{R}(n)\|_{\mathcal{H}} \leq \widetilde{C}$ for all n up to $\mathcal{O}(\frac{1}{\varepsilon})$, then it follows that

$$\begin{aligned} &\left\| \widetilde{\boldsymbol{U}}(n+1) - \boldsymbol{U}(n+1) \right\|_{\mathcal{H}} \\ &\leq (\lambda + \varepsilon\kappa L) \left\| \widetilde{\boldsymbol{U}}(n) - \boldsymbol{U}(n) \right\|_{\mathcal{H}} + \varepsilon^{m+1}\widetilde{C}. \end{aligned} \tag{60}$$

The derived difference inequality yields the estimate:

$$\begin{aligned} \left\| \widetilde{\boldsymbol{U}}(n) - \boldsymbol{U}(n) \right\|_{\mathcal{H}} \leq &(\lambda + \varepsilon\kappa L)^n \left\| \widetilde{\boldsymbol{U}}(0) - \boldsymbol{U}(0) \right\|_{\mathcal{H}} \\ &+ \varepsilon^{m+1}\widetilde{C}\frac{(\lambda + \varepsilon\kappa L)^n - 1}{\lambda + \varepsilon\kappa L - 1}. \end{aligned} \tag{61}$$

Case I: $0 < \lambda < 1$

We rewrite the powers as

$$\begin{aligned} &\left\| \widetilde{\boldsymbol{U}}(n) - \boldsymbol{U}(n) \right\|_{\mathcal{H}} \\ &\leq \underbrace{\lambda^n \left(1 + \varepsilon\frac{\kappa L}{\lambda}\right)^n}_{=\mathcal{O}(\lambda^n e^{\varepsilon n \frac{\kappa L}{\lambda}})} \left\| \widetilde{\boldsymbol{U}}(0) - \boldsymbol{U}(0) \right\|_{\mathcal{H}} \\ &+ \varepsilon^{m+1}\widetilde{C} \underbrace{\frac{\lambda^n \left(1 + \varepsilon\frac{\kappa L}{\lambda}\right)^n - 1}{\lambda + \varepsilon\kappa L - 1}}_{=\mathcal{O}\left(\lambda^n e^{\varepsilon n \frac{\kappa L}{\lambda}}\right)} \end{aligned} \tag{62}$$

$$\begin{aligned} &= \mathcal{O}\left(\lambda^n e^{\varepsilon n \frac{\kappa L}{\lambda}}\right) \left\| \widetilde{\boldsymbol{U}}(0) - \boldsymbol{U}(0) \right\|_{\mathcal{H}} \\ &+ \mathcal{O}\left(\varepsilon^{m+1}\lambda^n e^{\varepsilon n \frac{\kappa L}{\lambda}}\right). \end{aligned} \tag{63}$$

Assuming the initial condition satisfies

$$\left\| \widetilde{\boldsymbol{W}}(0) - \boldsymbol{W}(0) \right\|_{\mathcal{H}} = \mathcal{O}(\varepsilon^{m+1}), \tag{64}$$

where $\boldsymbol{U}(n) = P^{-1}\boldsymbol{W}(n)$, we conclude that for $n = \mathcal{O}(\frac{1}{\varepsilon})$:

$$\left\| \widetilde{\boldsymbol{W}}(n) - \boldsymbol{W}(n) \right\|_{\mathcal{H}} = \mathcal{O}(\varepsilon^{m+1}\lambda^n). \tag{65}$$

On the other hand, if we assume $\lambda = 1 - \varepsilon$, Eq.(62) yields to

$$\begin{aligned} &\left\| \widetilde{\boldsymbol{U}}(n) - \boldsymbol{U}(n) \right\|_{\mathcal{H}} \\ &\leq \lambda^n (1 + \varepsilon\frac{\kappa L}{\lambda})^n \left\| \widetilde{\boldsymbol{U}}(0) - \boldsymbol{U}(0) \right\|_{\mathcal{H}} \\ &+ \varepsilon^m \widetilde{C} \frac{\lambda^n (1 + \varepsilon\frac{\kappa L}{\lambda})^n - 1}{\kappa L - 1} \end{aligned} \tag{66}$$

$$\begin{aligned} &= \mathcal{O}(\lambda^n e^{\varepsilon n \frac{\kappa L}{\lambda}}) \left\| \widetilde{\boldsymbol{U}}(0) - \boldsymbol{U}(0) \right\|_{\mathcal{H}} \\ &+ \mathcal{O}(\varepsilon^m \lambda^n e^{\varepsilon n \frac{\kappa L}{\lambda}}). \end{aligned} \tag{67}$$

Hence, for the initial conditions (64), we conclude for iteration scale $n = \mathcal{O}(\frac{1}{\varepsilon})$:

$$\left\| \widetilde{\boldsymbol{W}}(n) - \boldsymbol{W}(n) \right\|_{\mathcal{H}} = \mathcal{O}(\varepsilon^m \lambda^n). \tag{68}$$

Case II: $\lambda = 1$

Where $(1+x)^n \le e^{nx}$ for $x > 0$, the estimate (61) becomes

$$\begin{aligned}\left\|\widetilde{\boldsymbol{U}}(n)-\boldsymbol{U}(n)\right\|_{\mathcal{H}} \le & \underbrace{(1+\varepsilon\kappa L)^n}_{=\mathcal{O}(e^{\varepsilon n\kappa L})}\left\|\widetilde{\boldsymbol{U}}(0)-\boldsymbol{U}(0)\right\|_{\mathcal{H}} \\ & +\varepsilon^m\widetilde{C}\underbrace{\frac{(1+\varepsilon\kappa L)^n-1}{\kappa L}}_{=\mathcal{O}(e^{\varepsilon n\kappa L})} \qquad (69)\\ =&\mathcal{O}(e^{\varepsilon n\kappa L})\left\|\widetilde{\boldsymbol{U}}(0)-\boldsymbol{U}(0)\right\|_{\mathcal{H}} \\ & +\mathcal{O}(\varepsilon^m e^{\varepsilon n\kappa L}). \qquad (70)\end{aligned}$$

Assuming the initial condition satisfies

$$\left\|\widetilde{\boldsymbol{W}}(0)-\boldsymbol{W}(0)\right\|_{\mathcal{H}} = \mathcal{O}\left(\varepsilon^m\right),$$

where $\boldsymbol{U}(n) = P^{-1}\boldsymbol{W}(n)$, we conclude that for $n = \mathcal{O}(\frac{1}{\varepsilon})$:

$$\left\|\widetilde{\boldsymbol{W}}(n)-\boldsymbol{W}(n)\right\|_{\mathcal{H}} = \mathcal{O}\left(\varepsilon^m\right). \qquad (71)$$

Case III: $\lambda > 1$

We define the rescaled variables

$$\begin{aligned}\boldsymbol{U}(n) &= \lambda^n\boldsymbol{V}(n),\\ \widetilde{\boldsymbol{U}}(n) &= \lambda^n\widetilde{\boldsymbol{V}}(n),\end{aligned} \qquad (72)$$

so that Eq. (57) becomes

$$\begin{aligned}\boldsymbol{V}(n+1) &= \frac{1}{\lambda}\Lambda\boldsymbol{V}(n)+\frac{\varepsilon}{\lambda^{n+1}}P^{-1}\boldsymbol{F}(\lambda^n P\boldsymbol{V}(n)),\\ \widetilde{\boldsymbol{V}}(n+1) &= \frac{1}{\lambda}\Lambda\widetilde{\boldsymbol{V}}(n)+\frac{\varepsilon}{\lambda^{n+1}}P^{-1}\boldsymbol{F}(\lambda^n P\widetilde{\boldsymbol{V}}(n))\\ &\quad +\frac{\varepsilon^{m+1}}{\lambda^{n+1}}P^{-1}\boldsymbol{R}(n).\end{aligned} \qquad (73)$$

Subtracting and applying $\mathcal{H}$-norm, we obtain

$$\begin{aligned}&\left\|\widetilde{\boldsymbol{V}}(n+1)-\boldsymbol{V}(n+1)\right\|_{\mathcal{H}}\\ &\le \frac{1}{\lambda}\|\Lambda\|\left\|\widetilde{\boldsymbol{V}}(n)-\boldsymbol{V}(n)\right\|_{\mathcal{H}}\\ &+\frac{\varepsilon}{\lambda^{n+1}}\left\|P^{-1}\right\|\left\|\boldsymbol{F}(\lambda^n P\boldsymbol{V}(n))+\boldsymbol{F}(\lambda^n P\widetilde{\boldsymbol{V}}(n))\right\|_{\mathcal{H}}\\ &+\frac{\varepsilon^{m+1}}{\lambda^{n+1}}\left\|P^{-1}\right\|\|\boldsymbol{R}(n)\|_{\mathcal{H}} \qquad (74)\\ &\le \left\|\widetilde{\boldsymbol{V}}(n)-\boldsymbol{V}(n)\right\|_{\mathcal{H}}\\ &+\frac{\varepsilon}{\lambda^{n+1}}\left\|P^{-1}\right\|\|P\|L\lambda^n\left\|\widetilde{\boldsymbol{V}}(n)-\boldsymbol{V}(n)\right\|_{\mathcal{H}}\\ &+\frac{\varepsilon^{m+1}}{\lambda^{n+1}}\widetilde{C} \qquad (75)\\ &= \left(1+\frac{\varepsilon\kappa L}{\lambda}\right)\left\|\widetilde{\boldsymbol{V}}(n)-\boldsymbol{V}(n)\right\|_{\mathcal{H}}+\frac{\varepsilon^{m+1}}{\lambda^{n+1}}\widetilde{C}. \qquad (76)\end{aligned}$$

Hence we obtain

$$\begin{aligned}\left\|\widetilde{\boldsymbol{V}}(n)-\boldsymbol{V}(n)\right\|_{\mathcal{H}} = & \underbrace{\left(1+\frac{\varepsilon\kappa L}{\lambda}\right)^n}_{=\mathcal{O}\left(e^{\frac{\varepsilon n\kappa L}{\lambda}}\right)}\left\|\widetilde{\boldsymbol{V}}(0)-\boldsymbol{V}(0)\right\|_{\mathcal{H}}\\ &+\underbrace{\frac{\varepsilon^m}{\lambda^n}\widetilde{C}\frac{\left(1+\frac{\varepsilon\kappa L}{\lambda}\right)^n-1}{\kappa L}}_{=\mathcal{O}\left(\frac{\varepsilon^m}{\lambda^n}e^{\frac{\varepsilon n\kappa L}{\lambda}}\right)}.\end{aligned} \qquad (77)$$

Assuming that

$$\left\|\widetilde{\boldsymbol{V}}(0)-\boldsymbol{V}(0)\right\|_{\mathcal{H}} = \mathcal{O}(\varepsilon^m),$$

we obtain for up to $n = \mathcal{O}(\frac{1}{\varepsilon})$ that

$$\left\|\widetilde{\boldsymbol{V}}(n)-\boldsymbol{V}(n)\right\|_{\mathcal{H}} = \mathcal{O}(\varepsilon^m). \qquad (78)$$

Recalling that $\boldsymbol{W}(n) = \lambda^n P\boldsymbol{V}(n)$, it follows that

$$\left\|\widetilde{\boldsymbol{W}}(n)-\boldsymbol{W}(n)\right\|_{\mathcal{H}} = \mathcal{O}(\varepsilon^m\lambda^n). \qquad (79)$$

□

4 On a weakly nonlinear PDE

In this section, we apply the multiple time-scales perturbation method to a weakly nonlinear PDE of Rayleigh type:

$$u_{tt}-u_{xx}+u = \varepsilon\left(u_t-\frac{1}{3}u_t^3\right), \qquad (80)$$

for $x \in (0,1)$, $t > 0$, and $0 < \varepsilon \ll 1$, subject to homogeneous Dirichlet boundary conditions $u(t,0) = u(t,1) = 0$, and subject to initial conditions given by $u(0,x) = f(x)$ and $u_t(0,x) = g(x)$. Already in 1970 this problem was studied by using averaging methods in [25]. Here, we outline its analysis using the multiple time-scales framework, and in the following subsection we study its discrete analogues (that is, PΔEs) under both standard and nonstandard finite difference schemes.

4.1 A MTS approximation of the solution

We introduce the fast and slow time scales $t_0 = t$ and $t_1 = \varepsilon t$, and expand the solution of (80) as

$$u(x,t) = u_0(x,t_0,t_1)+\varepsilon u_1(x,t_0,t_1)+\mathcal{O}(\varepsilon^2).$$

Substituting this into Eq. (80) yields:

$$\begin{aligned}&(\partial_{t_0}^2 u_0 - \partial_x^2 u_0 + u_0) + \varepsilon(\partial_{t_0}^2 u_1 - \partial_x^2 u_1 + u_1)\\ &= -\varepsilon 2\partial_{t_1}\partial_{t_0} u_0 + \varepsilon[(\partial_{t_0} u_0) - \frac{1}{3}(\partial_{t_0} u_0)^3] + \mathcal{O}(\varepsilon^2).\end{aligned} \tag{81}$$

This expansion gives us the first two leading order equations:

$$\mathcal{O}(1): \quad \partial_{t_0}^2 u_0 - \partial_x^2 u_0 + u_0 = 0, \tag{82a}$$

$$\begin{aligned}\mathcal{O}(\varepsilon): \quad &\partial_{t_0}^2 u_1 - \partial_x^2 u_1 + u_1\\ &= -2\partial_{t_1}\partial_{t_0} u_0 + (\partial_{t_0} u_0) - \frac{1}{3}(\partial_{t_0} u_0)^3.\end{aligned} \tag{82b}$$

Solving Eq. (82a) by using the method separation of variables yields the eigenpairs

$$\lambda_k = \omega_k^2 = 1 + \pi^2 k^2, \quad \varphi_k(x) = \sin(\pi k x), \tag{83}$$

and the general solution

$$\begin{aligned}u_0(x, t_0, t_1) = \sum_{k=1}^{\infty} &[A_k(t_1)\cos(\omega_k t_0)\\ &+ B_k(t_1)\sin(\omega_k t_0)]\sin(\pi k x),\end{aligned} \tag{84}$$

where $A_k(t_1)$ and $B_k(t_1)$ are still arbitrary functions which can be used to avoid secular terms in u_1.

To avoid secular growth in u_1, the right-hand side of Eq. (82b) must be orthogonal to the kernel of L_0, which is spanned by $\{\sin(\omega_k t_0), \cos(\omega_k t_0)\}$. This leads to the condition that the modal amplitudes $A_k(t_1)$, $B_k(t_1)$ for $k \in \mathbb{N}$ have to satisfy:

$$\begin{aligned}\dot{A}_m =&\frac{1}{2}A_m + \frac{1}{32}A_m(A_m^2 + B_m^2)\omega_m^2\\ &- \frac{1}{8}A_m\sum_{k=1}^{\infty}(A_k^2 + B_k^2)\omega_k^2,\end{aligned} \tag{85a}$$

$$\begin{aligned}\dot{B}_m =&\frac{1}{2}B_m + \frac{1}{32}B_m(A_m^2 + B_m^2)\omega_m^2\\ &- \frac{1}{8}B_m\sum_{k=1}^{\infty}(A_k^2 + B_k^2)\omega_k^2.\end{aligned} \tag{85b}$$

(See [25] for a similar and detailed derivation.)

We introduce scaled polar functions for each mode:

$$\begin{aligned}\omega_m A_m(t_1) =& r_m(t_1)\cos(\alpha_m(t_1)),\\ \omega_m B_m(t_1) =& r_m(t_1)\sin(\alpha_m(t_1)),\end{aligned} \tag{86}$$

Table 1 Stability types and eigenvalues for each equilibrium point

Equilibrium (r_1, r_2)	λ_1	λ_2	**Type**
$(0, 0)$	$\frac{1}{2}$	$\frac{1}{2}$	Unstable Node
$\left(0, \frac{4}{\sqrt{3}}\right)$	-1	$-\frac{1}{6}$	Stable Node
$\left(\frac{4}{\sqrt{3}}, 0\right)$	-1	$-\frac{1}{6}$	Stable Node
$\left(\frac{4}{\sqrt{7}}, \frac{4}{\sqrt{7}}\right)$	-1	$\frac{1}{7}$	Saddle

$\forall m \in \mathbb{N}^+$, which transforms the scaled modal amplitude equations (86) into

$$\dot{r}_m = \frac{1}{2}r_m + \frac{1}{32}r_m^3 - \frac{1}{8}r_m\sum_{k}^{\infty} r_k^2, \tag{87a}$$

$$\dot{\alpha}_m = 0. \tag{87b}$$

Example 1 (A Two-Mode System) Assume that only initial energy of the system is present in the first two modes. The system (87a) reduces to

$$\dot{r}_1 = \frac{1}{2}r_1 + \frac{1}{32}r_1^3 - \frac{1}{8}r_1(r_1^2 + r_2^2), \tag{88a}$$

$$\dot{r}_2 = \frac{1}{2}r_2 + \frac{1}{32}r_2^3 - \frac{1}{8}r_2(r_1^2 + r_2^2). \tag{88b}$$

Solving $\dot{r}_1 = 0$ and $\dot{r}_2 = 0$ yields

$$\begin{aligned}&r_1 = 0 \text{ or } 16 = 3r_1^2 + 4r_2^2, \text{ and}\\ &r_2 = 0 \text{ or } 16 = 4r_1^2 + 3r_2^2,\end{aligned} \tag{89}$$

which yields the equilibrium points. Resulting equilibria and and their linearised stability are listed in Table 1:

We present the phase portrait of this system in Fig. 1. In § 4.2, we extend the same MTS approximations to the discretised PDE and derive its modal amplitude equations. Example 2 illustrates the resulting dynamics when only the the first two modes are initially excited. In § 4.3, we compare the continuous (Example 1) and discrete (Example 2) two-mode systems to assess the correspondence between their modal dynamics.

4.2 Discretisation of the PDE

We now analyse the weakly nonlinear PDE (80) using finite difference approximations. We discretise the spatial and temporal domains as $x_i = i\Delta x$ for $i = 0, 1, \ldots, M = \frac{1}{\Delta x}$, and $t_n = n\Delta t$ for $n \in \mathbb{N}$. We denote the discrete approximation of $u(x, t)$ by $U(i, n)$. Following the nonstandard finite difference framework, we replace the standard discretisations

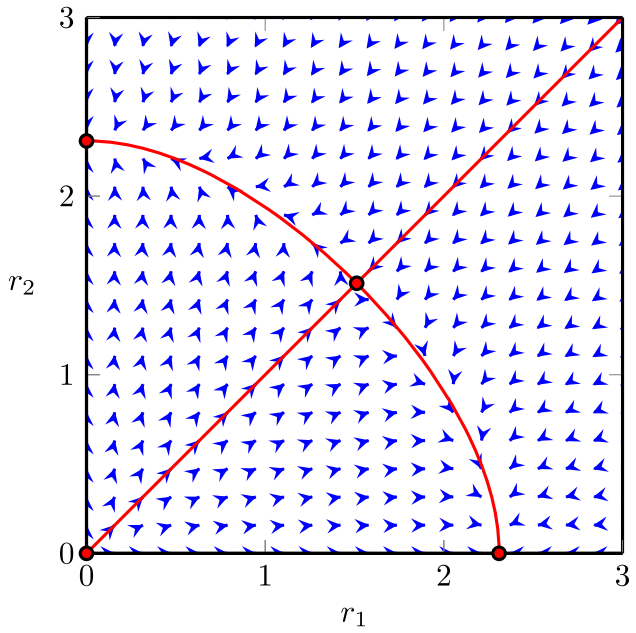

Fig. 1 Phase portrait of the two-mode system in scaled modal amplitudes (r_1, r_2) with equilibrium points ● and stable and unstable manifolds of the saddle ——.

with modified difference quotients:

$$\begin{aligned}(\Delta t)^2 \to \phi_t &= (\Delta t)^2 + \mathcal{O}((\Delta t)^2),\\ (\Delta x)^2 \to \phi_x &= (\Delta x)^2 + \mathcal{O}((\Delta x)^2),\\ 2\Delta t \to \psi_t &= 2\Delta t + \mathcal{O}(\Delta t),\end{aligned} \tag{90}$$

with $\phi_t, \phi_x, \psi_t > 0$, as originally proposed by Mickens in [19]. Following the operator-based notation introduced in Eq. (20) and (22), the discrete analogues of the differential operators become:

$$\begin{aligned}u_{tt} &\to \frac{\Delta_n^2 E_n^{-1} U(i,n)}{\phi_t},\\ u_{xx} &\to \frac{\Delta_i^2 E_i^{-1} U(i,n)}{\phi_x},\\ u_t &\to \frac{(\Delta_n^2 + 2\Delta_n) E_n^{-1} U(i,n)}{\psi_t}.\end{aligned} \tag{91}$$

Note that the numerators in (91) are equivalent to those in the standard discretisation (20). In the remainder of this section, we study the given equation under both the standard and nonstandard finite difference schemes by referring to ϕ_t, ϕ_x and ψ_t as standard or nonstandard quotients.

Using these approximations, the PΔE corresponding to Eq. (80) becomes:

$$\begin{aligned}&\frac{\Delta_n^2 U(i,n)}{\phi_t} - \frac{\Delta_i^2 E_i^{-1} E_n U(i,n)}{\phi_x} + E_n U(i,n) =\\ &\varepsilon\left(\frac{(\Delta_n^2 + 2\Delta_n)U(i,n)}{\psi_t} - \frac{\left[(\Delta_n^2 + 2\Delta_n)U(i,n)\right]^3}{3\psi_t^3}\right),\end{aligned} \tag{92}$$

accurate up to $\mathcal{O}((\Delta t)^2) + \mathcal{O}((\Delta x)^2)$, which we denote by the operator equation $LU = \varepsilon f(U)$.

Similarly as in § 2.3, we construct an approximation of the solution to Eq. (92) using multiple time-scales perturbation expansion. Introducing the fast and slow iteration scales

$$n_0(n) := n, \quad n_1(n) := \varepsilon n, \tag{93}$$

we expand the solution of the discrete problem Eq. (92) as:

$$U(i,n) = U_0(i, n_0, n_1) + \varepsilon U_1(i, n_0, n_1) + \mathcal{O}(\varepsilon^2). \tag{94}$$

Substituting this expansion into the discrete system, and using Eq. (9)-(12), we obtain the MTS expansion of $LU = f(U)$:

$$\begin{aligned}&(L_0 + L_1 + \mathcal{O}(\varepsilon^2))(U_0 + \varepsilon U_1 + \mathcal{O}(\varepsilon^2))\\ &= \varepsilon f_0(U_0 + \mathcal{O}(\varepsilon)) + \mathcal{O}(\varepsilon^2),\end{aligned} \tag{95}$$

which yields:

$$L_0 U_0 + \varepsilon L_0 U_1 + L_1 U_0 = \varepsilon f_0(U_0) + \mathcal{O}(\varepsilon^2). \tag{96}$$

The discrete operators involved are defined as:

$$\begin{aligned}L_0 &:= \frac{\Delta_{n_0}^2}{\phi_t} - \frac{\Delta_i^2 E_i^{-1} E_{n_0}}{\phi_x} + E_{n_0},\\ L_1 &:= \frac{2\Delta_{n_1}(\Delta_{n_0}^2 + \Delta_{n_0})}{\phi_t^2} - \frac{\Delta_i^2 \Delta_{n_1} E_{n_0}}{\phi_x^2},\\ f_0(\cdot) &:= \frac{(\Delta_{n_0}^2 + 2\Delta_{n_0})(\cdot)}{\psi_t} - \frac{[(\Delta_{n_0}^2 + 2\Delta_{n_0})(\cdot)]^3}{3\psi_t^3}.\end{aligned} \tag{97}$$

Since $\Delta_{n_1} = \mathcal{O}(\varepsilon)$, we obtain $L_1 = \mathcal{O}(\varepsilon)$ and following from (12), the leading-order equations are then:

$$\mathcal{O}(1): \quad L_0 U_0 = 0, \tag{98a}$$

$$\mathcal{O}(\varepsilon): \quad \varepsilon L_0 U_1 = -L_1 U_0 + \varepsilon f_0(U_0). \tag{98b}$$

To solve (98a), we use the method of separation of variables. Let

$$U_0(i, n_0, n_1) = V_0(n_0, n_1)\varphi(i). \tag{99}$$

Substituting this into Eq. (98a) gives

$$\begin{aligned}&\frac{\Delta_{n_0}^2 V_0(n_0,n_1)}{\phi_t}\varphi(i)\\&-\frac{(\Delta_i^2 E_i^{-1}\varphi(i))(E_{n_0}V_0(n_0,n_1))}{\phi_x}\\&+E_{n_0}V_0(n_0,n_1)\,\varphi(i)=0.\end{aligned}\tag{100}$$

By dividing both side by $E_{n_0}V_0(n_0,n_1)\,\varphi(i)$ and introducing a separation constant λ, we obtain:

$$\frac{(\Delta_{n_0}^2 V_0(n_0,n_1))}{\phi_t E_{n_0}V_0(n_0,n_1)}=\frac{(\Delta_i^2 E_i^{-1}\varphi(i))}{\phi_x\varphi(i)}-1=-\lambda.\tag{101}$$

This leads to the separated spatial and temporal problems.

Spatial problem and eigenvalues The spatial problem becomes

$$\begin{aligned}&(\Delta_i^2 E_i^{-1})\varphi(i)+\phi_x(\lambda-1)\varphi(i)=0,\\&\text{with}\quad \varphi(0)=\varphi(1/\Delta x)=0.\end{aligned}\tag{102}$$

This leads to the characteristic roots:

$$r_{1,2}=1-\tfrac{\phi_x(\lambda-1)}{2}\pm j\sqrt{\phi_x(\lambda-1)-\tfrac{\phi_x^2(\lambda-1)^2}{4}},\tag{103}$$

when $\phi_x(\lambda-1)-\frac{\phi_x^2(\lambda-1)^2}{4}>0$. It turns out that for $\phi_x(\lambda-1)-\frac{\phi_x^2(\lambda-1)^2}{4}\le 0$, only trivial solutions will be found. Hence, for nontrivial solutions, given inequality leads to $1<\lambda<1+\frac{4}{\phi_x}$, $|r_{1,2}|=1$ and $\varphi(i)$ is given by:

$$\varphi(i)=c_1\cos(\theta_\lambda\Delta x\, i)+c_2\sin(\theta_\lambda\Delta x\, i),\tag{104}$$

for $i=1,2,\ldots,M=\frac{1}{\Delta x}$, where

$$\begin{aligned}\cos(\theta_\lambda\Delta x)&:=1-\frac{\phi_x(\lambda-1)}{2},\\\sin(\theta_\lambda\Delta x)&:=\sqrt{\phi_x(\lambda-1)-\frac{\phi_x^2(\lambda-1)^2}{4}}.\end{aligned}\tag{105}$$

Imposing the boundary conditions $\varphi(0)=\varphi(1/\Delta x)=0$ gives $c_1=0$ and $\theta_{\lambda_k}=\pi k$ for $k\in\mathbb{N}^+$, so the eigenfunctions become

$$\varphi_k(i)=\sin(\pi k\Delta x\, i),\quad \text{with } \lambda_k\in\left(1,1+\tfrac{4}{\phi_x}\right).\tag{106}$$

The eigenvalues λ_k easily follow from the first equation in Eq. (105). For $\theta_{\lambda_k}=k\pi$ we find

$$\begin{aligned}\lambda_k&=1+\tfrac{2}{\phi_x}(1-\cos(k\pi\Delta x))\\&=1+\tfrac{4}{\phi_x}\sin^2(\tfrac{k\pi\Delta x}{2}).\end{aligned}\tag{107}$$

Temporal problem The temporal part of the separated problem (101) reads:

$$\Delta_{n_0}^2 V_{0k}(n_0,n_1)+\lambda_k\phi_t E_{n_0}V_{0k}(n_0,n_1)=0.\tag{108}$$

Its characteristic roots are:

$$r_{1,2}=1-\frac{\phi_t\lambda_k}{2}\pm j\sqrt{\phi_t\lambda_k-\frac{\phi_t^2\lambda_k^2}{4}}.\tag{109}$$

Given $0<\lambda_k<\frac{4}{\phi_t}$, we have $|r_{1,2}|=1$. From the physical perspective, this is the necessary and sufficient condition on the eigenvalues that leads to oscillatory time solutions of the given system, which is the characteristic of solution obtained for $\varepsilon=0$ and the approximation obtained for $0<\varepsilon\ll 1$ for the continuous PDE. For this given interval of λ_k, define

$$\begin{aligned}\cos(\widetilde{\omega}_k\Delta t)&:=1-\frac{\phi_t\lambda_k}{2},\\\sin(\widetilde{\omega}_k\Delta t)&:=\sqrt{\phi_t\lambda_k-\frac{\phi_t^2\lambda_k^2}{4}},\end{aligned}\tag{110}$$

so that the general temporal solution becomes

$$\begin{aligned}V_{0k}(n_0,n_1)=&A_k(n_1)\cos(\widetilde{\omega}_k n_0\Delta t)\\&+B_k(n_1)\sin(\widetilde{\omega}_k n_0\Delta t).\end{aligned}\tag{111}$$

We refer to $\widetilde{\omega}_k$ as the k-th natural frequency of the PΔE.

Combining spatial and temporal solutions for all modes, such that $U_0(i,n_0,n_1)=\sum_{k=1}^{\infty}V_{0k}(n_0,n_1)\varphi_k(i)$, solution of $\mathcal{O}(1)$ problem (98a) can be obtained as

$$\begin{aligned}U_0(i,n_0,n_1)=\sum_{k\in\mathbb{N}^+}\big[&A_k(n_1)\cos(\widetilde{\omega}_k n_0\Delta t)\\&+B_k(n_1)\sin(\widetilde{\omega}_k n_0\Delta t)\big]\varphi_k(i).\end{aligned}\tag{112}$$

Where we are seeking for approximations of the solutions of the PΔEs (92), which satisfy for $\varepsilon=0$ the exact solution of the PDE-problem (80). For other choices of ϕ_t, ϕ_x and ψ_t we will not have exactly matching solutions for $\varepsilon=0$ properly.

Difference quotients for ϕ_x, ϕ_t and ψ_t

The separation constants λ_k depend on ϕ_x, and the natural frequencies ω_k depend on both ϕ_t and ϕ_x. Since ϕ_x and ϕ_t are not a priori fixed, we consider two main cases. Either ϕ_x and ϕ_t are equal to the standard step sizes, i.e., $\phi_x=(\Delta x)^2$ and $\phi_t=(\Delta t)^2$, or they are the exact (nonstandard) discretisation step sizes.

For the harmonic oscillator the standard discretisation is

$$\frac{y(n+1)-2y(n)+y(n-1)}{\phi_t}+\omega^2 y(n)=0,\tag{113}$$

where $\phi_t = (\Delta t)^2$, and in the nonstandard discretisation

$$\phi_t = \frac{4}{\omega^2}\sin^2\left(\frac{\omega\Delta t}{2}\right) \tag{114}$$

[19]. Following this approach in Eq. (102) yields for each mode

$$\phi_x \to \phi_{x,k} = \frac{4}{\pi^2 k^2}\sin^2\left(\frac{\pi k\Delta x}{2}\right) \tag{115}$$

which gives eigenvalues:

$$\lambda_k = \begin{cases} 1 + \frac{4}{(\Delta x)^2}\sin^2(\frac{k\pi\Delta x}{2}) & \text{if} \quad \phi_x = (\Delta x)^2, \\ 1 + \pi^2 k^2 & \text{if} \quad \phi_{x,k} = \frac{4}{\pi^2 k^2}\sin^2(\frac{\pi k\Delta x}{2}). \end{cases} \tag{116}$$

Thus, the nonstandard eigenvalues λ_k (and as will be shown, eigenfrequencies $\widetilde{\omega}_k$) coincide with those from the continuous PDE (80).

Similarly for the temporal problem Eq. (108), the nonstandard expression can be obtained as

$$\phi_t \to \phi_{t,k} = \frac{4}{\widetilde{\omega}_k^2}\sin^2\left(\frac{\widetilde{\omega}_k\Delta t}{2}\right). \tag{117}$$

This leads to two scenarios for the natural frequencies:

If $\phi_x = (\Delta x)^2$ and $\phi_t = (\Delta t)^2$, we have the following expression for the natural frequencies,

$$\widetilde{\omega_k} = \tfrac{1}{\Delta t}\arcsin\Bigg[\left(1 + \tfrac{4}{(\Delta x)^2}\sin^2\left(\tfrac{\pi k\Delta x}{2}\right)\right)(\Delta t)^2 - \left(1 + \tfrac{4}{(\Delta x)^2}\sin^2\left(\tfrac{\pi k\Delta x}{2}\right)\right)^2 \tfrac{(\Delta t)^4}{4}\Bigg]^{\frac{1}{2}}. \tag{118}$$

If $\phi_x = \frac{4}{\pi^2 k^2}\sin^2(\frac{\pi k\Delta x}{2})$ and $\phi_t = \frac{4}{\widetilde{\omega}_k^2}\sin^2(\frac{\widetilde{\omega}_k\Delta t}{2})$, so choosing nonstandard discretisations for both time and space, we obtain the expression

$$\widetilde{\omega_k} = \sqrt{1 + \pi^2 k^2}. \tag{119}$$

This last natural frequency expression (119) is identical to the natural frequencies from the MTS expansion of the corresponding PDE (80).

Note that the choice of ϕ_x does not affect the eigenfunctions $\varphi(i)$, but it affects the eigenvalues λ_k, thus $\widetilde{\omega_k}$. Hence, the standard difference discretisations for ϕ_x and ϕ_t lead to a deviation the natural frequencies.

To compute the nonlinear term $f_0(U_0)$ in the $\mathcal{O}(\varepsilon)$ problem, we also require a nonstandard discretisation with ψ_t, which appears in the denominator of the first-order time difference operator defined in Eq. (90).

Consider a single mode of the solution:

$$\begin{aligned} V_{0m}(n_0, n_1) =& A_m(n_1)\cos(\widetilde{\omega_m} n_0\Delta t) \\ &+ B_m(n_1)\sin(\widetilde{\omega_m} n_0\Delta t). \end{aligned} \tag{120}$$

We assume that the discretisation of the nonstandard difference operator for first order time derivative near the time step n_0 is of the form:

$$\frac{(d_0 + d_{+1}E^1_{n_0} + d_{-1}E^{-1}_{n_0} + \dots)V_{0m}(n_0, n_1)}{\psi_t} \tag{121}$$

where d_l corresponds to the weights of neighboring cells of $V_{0m}(n_0, \cdot)$, and l represents the constant distance of neighboring cells on the positive iteration axis. We consider a 3 point stencil as an initial guess for the nonstandard first order difference operator. We compute the continuous derivative of the solution $V_{0m}(t_0, n_1)$ with respect to the fast scale $t_0 = n_0\Delta t$. This derivative serves as a reference expression that the discrete operator (121) should reproduce. In other words, we are using the exact derivative as a calibration tool to determine the correct discretisation ψ_t in the nonstandard finite difference operator. This leads to

$$\begin{aligned} \partial_{t_0} V_{0m}(t_0, n_1) =& \widetilde{\omega_m}\big(B_m(n_1)\cos(\widetilde{\omega_m} t_0) \\ &- A_m(n_1)\sin(\widetilde{\omega_m} t_0)\big). \end{aligned} \tag{122}$$

Again writing $n_0\Delta t$ for t_0 and matching coefficients of (121) and (122), we get

$$\begin{aligned} &\widetilde{\omega_m}\psi_{t,m}(B_m\cos(\widetilde{\omega_m} n_0\Delta t) - A_m\sin(\widetilde{\omega_m} n_0\Delta t)) \\ &= \cos(\widetilde{\omega_m} n_0\Delta t)\Big\{d_0 A_m \\ &\quad + d_{+1}[A_m\cos(\widetilde{\omega_m}\Delta t) + B_m\sin(\widetilde{\omega_m}\Delta t)] \\ &\quad + d_{-1}[A_m\cos(\widetilde{\omega_m}\Delta t) - B_m\sin(\widetilde{\omega_m}\Delta t)]\Big\} \\ &+ \sin(\widetilde{\omega_m} n_0\Delta t)\Big\{d_0 B_m \\ &\quad + d_{+1}[B_m\cos(\widetilde{\omega_m}\Delta t) - A_m\sin(\widetilde{\omega_m}\Delta t)] \\ &\quad + d_{-1}[B_m\cos(\widetilde{\omega_m}\Delta t) + A_m\sin(\widetilde{\omega_m}\Delta t)]\Big\}. \end{aligned} \tag{123}$$

From orthogonality, matching the coefficients of $\cos(\widetilde{\omega_m}\Delta t\, n_0)$ and $\sin(\widetilde{\omega_m}\Delta t\, n_0)$ terms, we obtain the necessary constraints:

$$\widetilde{\omega_m}\psi_{t,m} - (d_{+1} - d_{-1})\sin(\widetilde{\omega_m}\Delta t) = 0, \tag{124a}$$

$$d_0 + (d_{+1} + d_{-1})\cos(\widetilde{\omega_m}\Delta t) = 0. \tag{124b}$$

Assuming that $d_0, d_{\pm 1}$ are constants independent from mode number m and temporal step size Δt, then we find from (124b)

$$d_0 = 0, \text{ and } d_{-1} = -d_{+1}. \tag{125}$$

Choosing $d_{+1} = 1$ without loss of generality, we obtain

$$\psi_{t,m} = \tfrac{2}{\widetilde{\omega_m}} \sin(\widetilde{\omega_m}\Delta t). \tag{126}$$

Thus, as with $\phi_{x,k}$ and $\phi_{t,k}$, the discretisation size $\psi_{t,m}$ depends on the mode number m.

Spectral projection of the $\mathcal{O}(\varepsilon)$-problem

We now proceed to the $\mathcal{O}(\varepsilon)$-problem (98b), employing the spectral decomposition established previously. This step involves *spectral projection*, where the full system is projected onto the eigenbasis φ_k, allowing us to isolate the evolution equations for each modal amplitude.

Taking the inner product of both sides of Eq. (98b) with the m-th eigenfunction φ_m, we obtain

$$\varepsilon\langle L_0 U_1, \varphi_m\rangle = -\langle L_1 U_0, \varphi_m\rangle + \varepsilon\langle f_0(U_0), \varphi_m\rangle. \tag{127}$$

Assuming the modal expansion $U_1(i, n_0, n_1) = \sum_{k=1}^{\infty} V_{1k}(n_0, n_1)\varphi_k(i)$, and following similar calculations as for Eq. (38-(41)), we define

$$\begin{aligned} H_k(n_0, n_1) &:= (\Delta_{n_0}^2 + 2\Delta_{n_0})V_{0k}(n_0, n_1) \\ &= F_m(n_1)\cos(\widetilde{\omega_m} n_0 \Delta t) + G_m(n_1)\sin(\widetilde{\omega_m} n_0 \Delta t). \end{aligned} \tag{128}$$

where $F_m(n_1)$ and $G_m(n_1)$ are defined as

$$\begin{aligned} F_m(n_1) :=& A_m(n_1)\cos(2\widetilde{\omega_m}\Delta t) \\ &+ B_m(n_1)\sin(2\widetilde{\omega_m}\Delta t) - A_m(n_1), \end{aligned} \tag{129a}$$

$$\begin{aligned} G_m(n_1) :=& -A_m(n_1)\sin(2\widetilde{\omega_m}\Delta t) \\ &+ B_m(n_1)\cos(2\widetilde{\omega_m}\Delta t) - B_m(n_1). \end{aligned} \tag{129b}$$

Substituting Eq. (128) into Eq. (127), we obtain the evolution equation for V_{1m}:

$$\begin{aligned} &\varepsilon\left(\frac{\Delta_{n_0}^2}{\phi_{t,m}} + \lambda_m E_{n_0}\right) V_{1m} \\ &= -\frac{\Delta_{n_1} H_m}{\phi_{t,m}} + \varepsilon\frac{H_m}{\psi_{t,m}} \\ &\quad - \varepsilon\frac{2}{3}\sum_k\sum_p\sum_q \frac{H_k H_p H_q}{\psi_{t,k}\psi_{t,p}\psi_{t,q}}\langle\varphi_k\varphi_p\varphi_q, \varphi_m\rangle. \end{aligned} \tag{130}$$

Avoiding secular terms

To avoid secular growth in $V_{1m}(n_0, n_1)$, the right-hand side of (130) must be orthogonal to the kernel of the operator on the left-hand side, which is spanned by $\{\sin(\widetilde{\omega_k}\Delta t\, n_0), \cos(\widetilde{\omega_k}\Delta t\, n_0)\}$. Retaining only resonant contributions, we obtain the secular terms:

$$\begin{aligned} &\varepsilon\left(\frac{\Delta_{n_0}^2}{\phi_{t,m}} + \lambda_m E_{n_0}\right) V_{1m}(n_0, n_1) \\ &= -\frac{\Delta_{n_1} H_m(n_0, n_1)}{\phi_{t,m}} + \varepsilon\frac{H_m(n_0, n_1)}{\psi_{t,m}} \\ &\quad - \varepsilon\frac{1}{8}\left(\frac{H_m^3(n_0, n_1)}{\psi_{t,m}^3} \right. \\ &\qquad \left. + 2\sum_{k\neq m}^{\infty}\frac{H_k^2(n_0, n_1)H_m(n_0, n_1)}{\psi_{t,k}^2\psi_{t,m}}\right) + \text{n.r.t.} \end{aligned} \tag{131}$$

where "n.r.t" stands for non-resonant terms. The details on the reduction of the triple summation and the identification of resonant contributions are presented in the Appendix A. The secular terms can be avoided if

$$\begin{aligned} &\Delta_{n_1} H_m(n_0, n_1) \\ &= \varepsilon\tfrac{\phi_{t,m}}{2\psi_{t,m}} H_m(n_0, n_1) - \varepsilon\tfrac{\phi_{t,m}}{8\psi_{t,m}^3} H_m^3(n_0, n_1) \\ &\quad - \varepsilon\tfrac{\phi_{t,m}}{4\psi_{t,m}} H_m(n_0, n_1)\sum_{k\neq m}^{\infty}\tfrac{1}{\psi_{t,k}^2} H_k^2(n_0, n_1). \end{aligned} \tag{132}$$

As a result, the evolution of the modal components F_m and G_m becomes:

$$\begin{aligned} &E_{n_1} F_m(n_1) = \\ &\left(1 + \varepsilon\tfrac{\phi_{t,m}}{2\psi_{t,m}}\right) F_m(n_1) \\ &+ \varepsilon\tfrac{\phi_{t,m}}{32\psi_{t,m}^3} F_m(n_1)(F_m^2(n_1) + G_m^2(n_1)) \\ &- \varepsilon\tfrac{\phi_{t,m}}{8\psi_{t,m}} F_m(n_1)\sum_{k=1}^{\infty}\tfrac{(F_k^2(n_1)+G_k^2(n_1))}{\psi_{t,k}^2}, \end{aligned} \tag{133a}$$

$$\begin{aligned} &E_{n_1} G_m(n_1) = \\ &\left(1 + \varepsilon\tfrac{\phi_{t,m}}{2\psi_{t,m}}\right) G_m(n_1) \\ &+ \varepsilon\tfrac{\phi_{t,m}}{32\psi_{t,m}^3} G_m(n_1)(F_m^2(n_1) + G_m^2(n_1)) \\ &- \varepsilon\tfrac{\phi_{t,m}}{8\psi_{t,m}} G_m(n_1)\sum_{k=1}^{\infty}\tfrac{(F_k^2(n_1)+G_k^2(n_1))}{\psi_{t,k}^2}. \end{aligned} \tag{133b}$$

Introducing polar coordinates

$$\begin{aligned} F_m(n_1) &= \rho_m(n_1)\cos(\beta_m(n_1)), \\ G_m(n_1) &= \rho_m(n_1)\sin(\beta_m(n_1)), \end{aligned} \tag{134}$$

$\forall m \in \mathbb{N}^+$, for (133*a*) $\times \cos(\beta_m) +$ (133*b*) $\times \sin(\beta_m)$ equates to

$$\begin{aligned}
&(E_{n_1}\rho_m(n_1))\big[\cos(E_{n_1}\beta_m(n_1))\cos(\beta_m(n_1)) \\
&\qquad + \sin(E_{n_1}\beta_m(n_1))\sin(\beta_m(n_1))\big] \\
&= (E_{n_1}\rho_m(n_1))\cos(\Delta_\varepsilon\beta_m(n_1)) \\
&= (1+\varepsilon\tfrac{\phi_{t,m}}{2\psi_{t,m}})\rho_m(n_1) + \varepsilon\tfrac{\phi_{t,m}}{32\psi_{t,m}^3}\rho_m^3(n_1) \\
&- \varepsilon\tfrac{\phi_{t,m}}{8\psi_{t,m}}\rho_m(n_1)\sum_{k=1}^{\infty}\tfrac{\rho_k^2(n_1)}{\psi_{t,k}^2},
\end{aligned} \tag{135}$$

and from (133*b*) $\times \cos(\beta_m) -$ (133*a*) $\times \sin(\beta_m)$ we have

$$\begin{aligned}
&(E_{n_1}\rho_m(n_1))\big[\sin(E_{n_1}\beta_m(n_1))\cos(\beta_m(n_1)) \\
&+ \sin(E_{n_1}\beta_m(n_1))\cos(\beta_m(n_1))\big] \\
&= (E_{n_1}\rho_m(n_1))\sin(\Delta_{n_1}\beta_m(n_1)) = 0.
\end{aligned} \tag{136}$$

Notice that $E_{n_1}\rho_m(n_1) = 0 \Leftrightarrow \rho_m(n_1) = 0$ for all modes m, and slow iterations n_1, i.e. the trivial solution. Hence, The only nontrivial solution for Eq. (136) is that $\Delta_{n_1}\beta_m(n_1) = 0$ or $\Delta_{n_1}\beta_m(n_1) = l\pi$, $l \in \mathbb{N}^+$ hence we obtain

$$\begin{aligned}
E_{n_1}\rho_m(n_1) &= \left(1+\varepsilon\tfrac{\phi_{t,m}}{2\psi_{t,m}}\right)\rho_m(n_1) + \varepsilon\tfrac{\phi_{t,m}}{32\psi_{t,m}^3}\rho_m^3(n_1) \\
&\quad - \varepsilon\tfrac{\phi_{t,m}}{8\psi_{t,m}}\rho_m(n_1)\sum_{k=1}^{\infty}\tfrac{\rho_k^2(n_1)}{\psi_{t,k}^2},
\end{aligned} \tag{137a}$$

$$E_{n_1}\beta_m(n_1) = 0. \tag{137b}$$

This indicates no phase shift for modal frequencies, and the dynamics are

Example 2 (2 modes) Consider initial energy only in the first two modes:

$$\begin{aligned}
\rho_1(\varepsilon n+\varepsilon) &= \left(1+\varepsilon\tfrac{\phi_{t,1}}{2\psi_{t,1}}\right)\rho_1 + \varepsilon\tfrac{\phi_{t,1}}{32\psi_{t,1}^3}\rho_1^3 \\
&\quad - \varepsilon\tfrac{\phi_{t,1}}{8\psi_{t,1}}\rho_1\left(\tfrac{\rho_1^2}{\psi_{t,1}^2} + \tfrac{\rho_2^2}{\psi_{t,2}^2}\right),
\end{aligned} \tag{138a}$$

$$\begin{aligned}
\rho_2(\varepsilon n+\varepsilon) &= (1+\varepsilon\tfrac{\phi_{t,2}}{2\psi_{t,2}})\rho_2 + \tfrac{\phi_{t,2}}{32\psi_{t,2}^3}\rho_2^3 \\
&\quad - \tfrac{\phi_{t,2}}{8\psi_{t,2}}\rho_2\left(\tfrac{\rho_1^2}{\psi_{t,1}^2} + \tfrac{\rho_2^2}{\psi_{t,2}^2}\right).
\end{aligned} \tag{138b}$$

The fixed points are determined as follows. For (138a):

$$\rho_1 = 0 \text{ or } 3\tfrac{\rho_1^2}{\psi_{t,1}^2} + 4\tfrac{\rho_2^2}{\psi_{t,2}^2} = 16, \tag{139}$$

and for (138b):

$$\rho_2 = 0 \text{ or } 4\tfrac{\rho_1^2}{\psi_{t,1}^2} + 3\tfrac{\rho_2^2}{\psi_{t,2}^2} = 16. \tag{140}$$

Table 2 Stability types and eigenvalues for each fixed point

Fixed point(ρ_1, ρ_2)	μ_1	μ_2	**Type**
$(0, 0)$	$1+\varepsilon\frac{\phi_{t,1}}{2\psi_{t,1}}$	$1+\varepsilon\frac{\phi_{t,2}}{2\psi_{t,2}}$	Unstable Node
$\left(0, \frac{4\psi_{t,2}}{\sqrt{3}}\right)$	$1-\varepsilon\frac{\phi_{t,1}}{6\psi_{t,1}}$	$1-\varepsilon\frac{\phi_{t,2}}{\psi_{t,2}}$	Stable Node
$\left(\frac{4\psi_{t,1}}{\sqrt{3}}, 0\right)$	$1-\varepsilon\frac{\phi_{t,1}}{\psi_{t,1}}$	$1-\varepsilon\frac{\phi_{t,2}}{6\psi_{t,2}}$	Stable Node
$\left(\frac{4\psi_{t,1}}{\sqrt{7}}, \frac{4\psi_{t,2}}{\sqrt{7}}\right)$	$1-\varepsilon\eta_1$	$1+\varepsilon\eta_2$	Saddle

This yields the fixed points:

$$\begin{aligned}
&\rho_1 = 0, \quad \rho_2 = 0, \\
&\rho_1 = 0, \quad \rho_2 = \tfrac{4}{\sqrt{3}}\psi_{t,2}, \\
&\rho_1 = \tfrac{4}{\sqrt{3}}\psi_{t,1}, \quad \rho_2 = 0, \\
&\rho_1 = \tfrac{4}{\sqrt{7}}\psi_{t,1}, \quad \rho_2 = \tfrac{4}{\sqrt{7}}\psi_{t,2}.
\end{aligned} \tag{141}$$

We determine the linear stability, following the eigenvalues, of each fixed point in Table 2:

where

$$\begin{aligned}
\eta_1 &:= \tfrac{3(\phi_{t,1}\psi_{t,2}+\phi_{t,2}\psi_{t,1})}{14\psi_{t,1}\psi_{t,2}} \\
&\quad + \tfrac{\sqrt{9\phi_{t,1}^2\psi_{t,2}^2+46\phi_{t,1}\psi_{t,2}\phi_{t,2}\psi_{t,1}+9\phi_{t,2}^2\psi_{t,1}^2}}{14\psi_{t,1}\psi_{t,2}}, \\
\eta_2 &:= \tfrac{-3(\phi_{t,1}\psi_{t,2}+\phi_{t,2}\psi_{t,1})}{14\psi_{t,1}\psi_{t,2}} \\
&\quad + \tfrac{\sqrt{9\phi_{t,1}^2\psi_{t,2}^2+46\phi_{t,1}\psi_{t,2}\phi_{t,2}\psi_{t,1}+9\phi_{t,2}^2\psi_{t,1}^2}}{14\psi_{t,1}\psi_{t,2}},
\end{aligned} \tag{142}$$

and notice that $\eta_{1,2} > 0$.

Having obtained the MTS approximations for both the continuous PDE and its standard and nonstandard discretisations, it is essential to examine how these approximations relate to one another. It is crucial to determine whether the discrete systems reproduce the same equilibria and stability behaviour as the continuous one, or whether additional features arise due to discretisation. To address these questions, we next compare the continuous and discrete MTS approximations in § 4.3, focusing on the two-mode examples.

4.3 Comparison of MTS for the PDE and the PΔE

We have derived the MTS approximation of the continuous PDE (80) in § 4.1, as well as the MTS approximation for the standard and nonstandard difference schemes in § 4.2. We now compare these approximations by studying the natural frequencies and fixed point structures in their 2-mode examples.

4.3.1 Natural frequencies

It is evident that the natural frequencies of the nonstandard PΔE is identical to those of the continuous PDE. Therefore, we focus on the standard difference scheme. Using the natural frequencies ω_k and $\widetilde{\omega_k}$ from the continuous PDE (83) and the standard PΔE (118), respectively, we compare them for each mode.

The relative difference between ω_k and $\widetilde{\omega_k}$ is computed by taking ω_k as the reference frequency for each mode. The results for the first two modes, showing the relative difference as a function of Δx and Δt, are presented in Fig. 2. It can be observed that for $\Delta x \simeq \Delta t$, a more accurate natural frequency approximation is achieved for the standard difference schemes.

4.3.2 Fixed points

Let us recall the definitions of ρ_m from (134) and r_m from (86), along with the definitions of F_m and G_m (129). These allow us to compare the fixed points of nonstandard and standard schemes of the PΔE with those of the continuous PDE.

Standard finite difference

First we consider the standard discretisation, where

$$\phi_{t,m} = \phi_t = (\Delta t)^2, \quad \psi_{t,m} = \psi_t = 2\Delta t$$

leading to the fixed points:

$$\begin{aligned} &\rho_1 = 0, \quad \rho_2 = 0, \\ &\rho_1 = 0, \quad \rho_2 = \tfrac{8\Delta t}{\sqrt{3}}, \\ &\rho_1 = \tfrac{8\Delta t}{\sqrt{3}}, \quad \rho_2 = 0, \\ &\rho_1 = \tfrac{8\Delta t}{\sqrt{7}}, \quad \rho_2 = \tfrac{8\Delta t}{\sqrt{7}}. \end{aligned} \tag{143}$$

From the discrete definition of ρ_m, we obtain

$$\begin{aligned} \rho_m &= \sqrt{F_m^2 + G_m^2} \\ &\overset{(129)}{=} 2\sqrt{A_m^2 + B_m^2}\, \underbrace{\sin(\widetilde{\omega_m}\Delta t)}_{\text{Eq. (118)}}. \end{aligned} \tag{144}$$

The modal amplitude can be then written as

$$\widetilde{R}_m = \sqrt{A_m^2 + B_m^2} = \frac{\rho_m}{2\sin(\widetilde{\omega_m}\Delta t)}. \tag{145}$$

On the other hand, following from Eq. (86), the modal amplitude for the continuous PDE is given by

$$R_m = \sqrt{A_m^2 + B_m^2} = \frac{r_m}{\omega_m}. \tag{146}$$

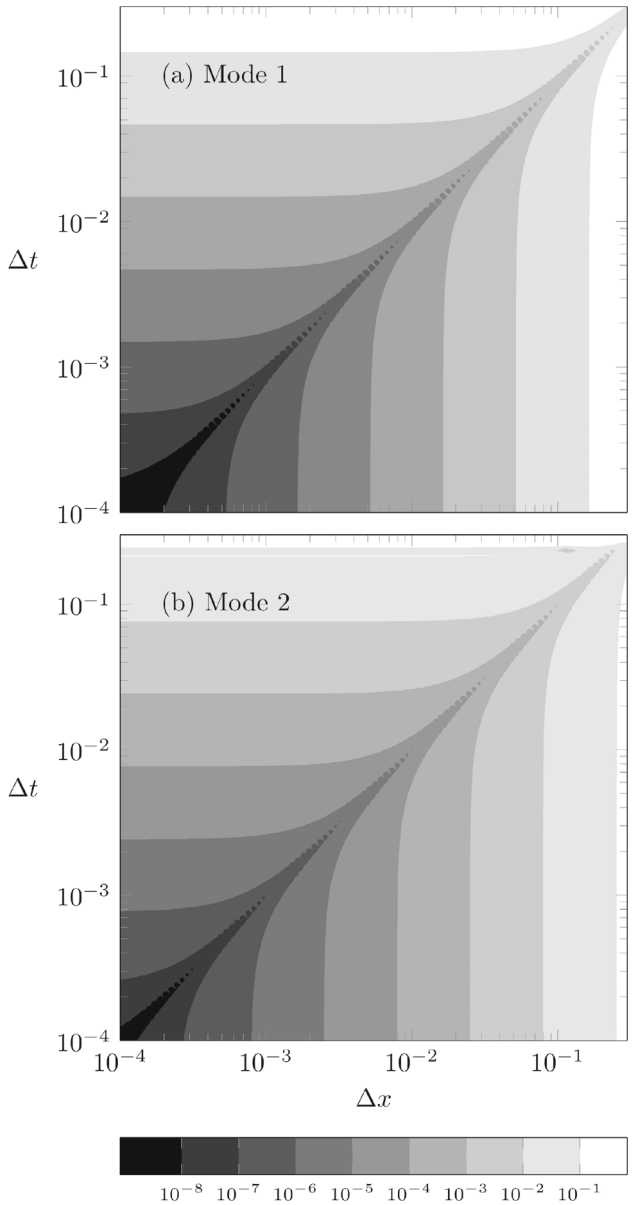

Fig. 2 Relative error $\frac{|\omega_m - \widetilde{\omega_m}|}{\omega_m}$, for $m = 1, 2$

Thus, the modal amplitudes $\sqrt{A_m^2 + B_m^2}$ serves as the natural measure to compare the fixed points of the standard and nonstandard schemes with those of the continuous PDE (80), see Table 3.

The relative error of the fixed points of the standard difference scheme modal amplitudes with respect to the continuous system are computed by $\frac{|R_m - \widetilde{R}_m|}{R_m}$.

Observe in Fig. 3 that refining only the temporal or only the spatial discretisation does not reduce the error in the fixed points of the modal amplitudes. Therefore, to achieve a better approximation, both Δx and Δt should be refined proportionally.

Table 3 Stability types and eigenvalues μ_m for each fixed point

Fixed Points	PDE			PΔE		
	(R_1, R_2)	μ_1	μ_2	$(\widetilde{R}_1, \widetilde{R}_2)$	μ_1	μ_2
Eqb-1	$(0, 0)$	$\frac{1}{2}$	$\frac{1}{2}$	$(0, 0)$	$1+\varepsilon\frac{\Delta t}{4}$	$1+\varepsilon\frac{\Delta t}{4}$
Eqb-2	$(0, \frac{4}{\sqrt{3}\omega_2})$	$-\frac{1}{6}$	-1	$(0, \frac{4\Delta t}{\sqrt{3}\sin(\widetilde{\omega}_2\Delta t)})$	$1-\varepsilon\frac{\Delta t}{12}$	$1-\varepsilon\frac{\Delta t}{2}$
Eqb-3	$(\frac{4}{\sqrt{3}\omega_1}, 0)$	-1	$-\frac{1}{6}$	$(\frac{4\Delta t}{\sqrt{3}\sin(\widetilde{\omega}_1\Delta t)}, 0)$	$1-\varepsilon\frac{\Delta t}{2}$	$1-\varepsilon\frac{\Delta t}{12}$
Eqb-4	$(\frac{4}{\sqrt{7}\omega_1}, \frac{4}{\sqrt{7}\omega_2})$	-1	$\frac{1}{7}$	$(\frac{4\Delta t}{\sqrt{7}\sin(\widetilde{\omega}_1\Delta t)}, \frac{4\Delta t}{\sqrt{7}\sin(\widetilde{\omega}_2\Delta t)})$	$1-\varepsilon\frac{\Delta t}{2}$	$1+\varepsilon\frac{\Delta t}{14}$

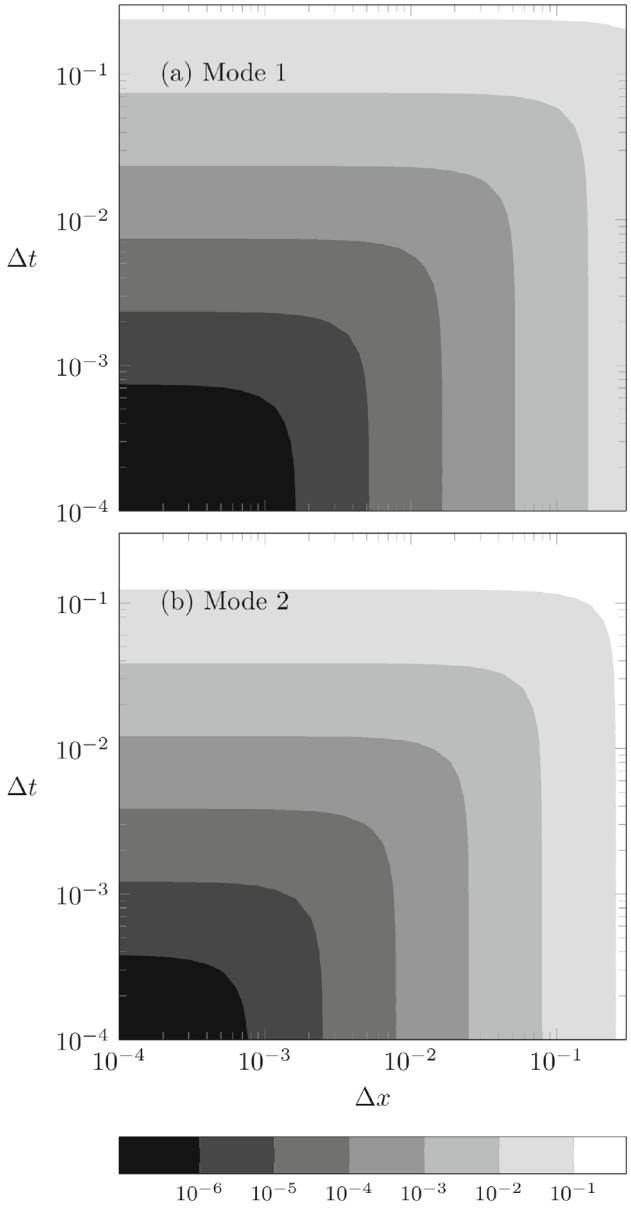

Fig. 3 Relative error $\frac{|R_m-\widetilde{R}_m|}{R_m}$, for $m = 1, 2$

Nonstandard finite difference

We now consider the nonstandard difference approach for the difference scheme with the following definitions:

$$\begin{aligned}\phi_{t,m} &= \frac{4}{\omega_m^2}\sin^2\left(\frac{\omega_m\Delta t}{2}\right),\\ \psi_{t,m} &= \frac{2}{\omega_m}\sin\left(\omega_m\Delta t\right)\end{aligned} \tag{147}$$

for each mode m. Using these definitions with (144), we find that for each fixed point, $(\widetilde{R}_1, \widetilde{R}_2) = (R_1, R_2)$, meaning the fixed points of the modal amplitudes coincide with those of the continuous PDE. Similarly, we have previously shown that the NSFD scheme yields natural frequencies in the PΔE that exactly match those of the corresponding continuous MTS approximation for the solution of the PDE.

5 Conclusion and discussion

In this study, the theory of the multiple time-scales perturbation method has been extended to initial-boundary value problems for partial difference equations (PΔEs). We have introduced discrete operators that include fast and slow iteration scales for PΔEs, extending earlier work on OΔEs to the spatially discrete case. Using these operators, multiple time-scales approximations for both a linear and a nonlinear PΔE have been derived from their corresponding continuous PDEs. The asymptotic validity of these approximations has been established in a Hilbert space setting, providing a rigorous foundation for the method.

A linear PDE example has been analysed to allow direct comparison between its exact solution, its multiple time-scales approximation in the continuous setting, and the multiple time-scales approximation of its discretised form. Subsequently, a weakly nonlinear PDE of Rayleigh type has been studied using both standard and nonstandard finite difference discretisations. The resulting multiple time-scales approximations for these schemes have been compared with those of the continuous PDE.

It has been observed that the eigenfunctions of the continuous PDE remain invariant under both standard and nonstandard PΔE discretisations. On the other hand, the eigenvalues are affected by the choice of the second-order

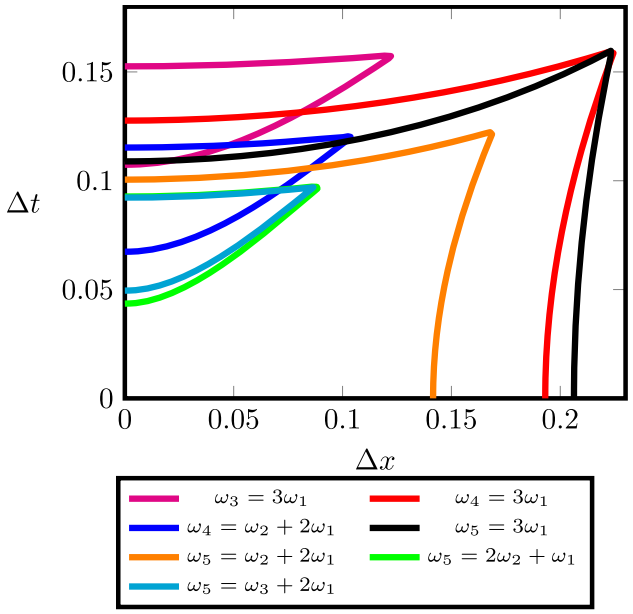

Fig. 4 Some examples for spurious resonance interactions in $(\Delta x, \Delta t)$

spatial difference operator. Standard spatial discretisation leads to eigenvalues that differ from those of the continuous system but converge to the exact values as the grid size becomes smaller. In contrast, the nonstandard discretisation yields eigenvalues that match exactly with those of the PDE for each mode, regardless of the grid size.

Similarly, the natural frequencies depend on the choice of both spatial and temporal second-order difference operators. Standard differences lead to approximations that converge to the exact natural frequencies as the grid is refined, while nonstandard discretisation yield natural frequencies that are identical to those of the continuous system for all modes. Consequently, the nonstandard discretisation reproduces the internal resonance structure of the continuous system exactly for all modes. For standard differences, the validity of the approximation is effectively limited to mode numbers up to $m \lesssim \frac{1}{2\Delta x}$, assuming $\Delta x \sim \Delta t \ll 1$.

Numerical results also indicate that standard discretisations may exhibit *spurious* resonance interactions. Although Appendix A proves that resonances of the form $\omega_m = \omega_k + \omega_p + \omega_q$ cannot occur, these spurious resonance interactions occur for certain pairs of $(\Delta x, \Delta t)$, as illustrated in Fig. 4. For instance, for $\Delta x = 0.05$ fixed, the spurious interaction $\omega_3 = 3\omega_1$ (for $m = 3$ and $k = p = q = 1$) arises at both $\Delta t = 0.1534$ and $\Delta t = 0.1171$, lying on the manifold represented by the curve —— in Fig. 4.

As a concrete example, a two-mode scenario has been analysed. It was shown that when there is no initial energy (up to $\mathcal{O}(\varepsilon)$ for times of $\mathcal{O}(\frac{1}{\varepsilon})$) in the remaining modes, they remain decoupled with zero energy due to the structure of the PDE. In this case, four modal equilibria were identified: an unstable trivial equilibrium, a saddle equilibrium, and two stable equilibria, each characterised by energy concentrated in a single mode. The locations of these nontrivial equilibria are influenced by the choice of the temporal first-order difference operator. The nonstandard scheme leads the same equilibria as for the continuous PDE's multiple time-scales approximations.

Overall, the nonstandard difference scheme yields the exact solution when $\varepsilon = 0$. For $0 < \varepsilon \ll 1$, it produces solutions that are identical to the multiple time-scales approximation of the continuous PDE. However, the nonstandard approach requires discretisations that depend on the mode number, which poses challenges for systems involving many strongly coupled modes.

Future work may focus on extending the proposed framework to higher-dimensional problems, more complicated boundary conditions, and a wider class of PDEs with their corresponding PΔEs. A direct extension of the present study is to consider equations with weakly space- and time-dependent coefficients and to investigate different types of weak nonlinearities. In addition, the occurrence of spurious resonance interactions in standard discretisations can be studied in further detail. Insights of the origins of spurious resonances could guide to development of difference schemes that suppress spurious resonances while preserving the actual modal structure of the continuous system.

Appendix A Modal interactions

In this appendix, we provide the intermediate steps leading from Eq. (130) to Eq. (133). We begin by restating Eq. (130):

$$\begin{aligned} &\varepsilon\left(\frac{\Delta_{n_0}^2}{\phi_{t,m}} + \lambda_m E_{n_0}\right) V_{1m} \\ &= -\frac{\Delta_{n_1} H_m}{\phi_{t,m}} + \varepsilon \frac{H_m}{\psi_{t,m}} \\ &\quad - \varepsilon \frac{2}{3} \sum_k \sum_p \sum_q \frac{H_k H_p H_q}{\psi_{t,k}\psi_{t,p}\psi_{t,q}} \langle \varphi_k \varphi_p \varphi_q, \varphi_m \rangle. \end{aligned} \tag{A1}$$

The nonlinear contributions to the modal interactions come from the inner product in the right-hand side of (A1). Using the orthogonality of the discrete cosine basis over the uniform grid with step size Δx, we obtain

$$\begin{aligned} &\langle \varphi_k \varphi_p \varphi_q, \varphi_m \rangle \\ &= \frac{\Delta x}{8} \sum_{i=0}^{1/\Delta x} \cos((k \pm p \pm q \pm m)\pi i \Delta x) \end{aligned} \tag{A2}$$

$$= \begin{cases} \frac{1}{8}, & \text{if } \pm k \pm p \pm q \pm m = 0, \\ 0, & \text{else,} \end{cases} \tag{A3}$$

where the summation is over all sign combinations. Substituting this into Eq. (A1), gives

$$\sum_k \sum_p \sum_q \frac{H_k H_p H_q}{\psi_{t,k}\psi_{t,p}\psi_{t,q}} \langle \varphi_k \varphi_p \varphi_q, \varphi_m \rangle \tag{A4}$$

$$\begin{aligned} =&\frac{1}{8}\Bigg(\sum_{m=-k+p+q} + \sum_{m=k-p+q} + \sum_{m=k+p-q} \\ &- \sum_{m=-k+p-q} - \sum_{m=-k-p+q} - \sum_{m=k-p-q} \\ &- \sum_{m=+k+p+q} + \sum_{m=-k-p-q} \Bigg) \frac{H_k H_p H_q}{\psi_{t,k}\psi_{t,p}\psi_{t,q}}. \end{aligned} \tag{A5}$$

The term with the summation over $m = -k - p - q$ vanish since $m, k, p, q \in \mathbb{N}^+$. Due to the symmetry over the indices, Eq. (A5) simplifies to:

$$\frac{3}{8}\Bigg(\sum_{m=-k+p+q} - \sum_{m=k-p-q} - \frac{1}{3} \sum_{m=k+p+q} \Bigg) \frac{H_k H_p H_q}{\psi_{t,k}\psi_{t,p}\psi_{t,q}}. \tag{A6}$$

To identify secular (resonant) contributions, we note that $\sin(\omega_m n)$ and $\cos(\omega_m n)$ lie in the kernel of left-hand operator in Eq. (130). The product $H_k H_p H_q$ generates combinations of the form $\sin((\pm\omega_k \pm \omega_p \pm \omega_q)n)$ and $\cos((\pm\omega_k \pm \omega_p \pm \omega_q)n)$, up to multiplicative constants. We therefore need to determine for which combinations of k, p, and q these resonant terms arise:

$$\omega_m = \pm\omega_k \pm \omega_p \pm \omega_q. \tag{A7}$$

In order to rule out or to determine secular terms, we impose the following assumptions on the natural frequencies $\{\omega_k\}_{k\in\mathbb{N}^+}$:

1. Frequencies are positive:

$$\omega_k > 0. \tag{Cond-1}$$

2. Frequencies are strictly increasing:

$$\Delta\omega_k = \omega_{k+1} - \omega_k > 0. \tag{Cond-2}$$

3. The frequency sequence is convex:

$$\Delta^2\omega_k = \omega_{k+2} - 2\omega_{k+1} + \omega_k > 0. \tag{Cond-3}$$

4. Frequencies are strictly sub-additive:

$$\omega_{k+m} < \omega_k + \omega_m. \tag{Cond-4}$$

5. Frequencies are linearly bounded:

$$\pi k < \omega_k < \pi(k + \tfrac{1}{2}). \tag{Cond-5}$$

While the first two conditions are natural, Conditions 3-5 require further justification, provided in Appendix B. Though these assumptions may seem strong, they become practical when analysing complex natural frequency expressions of the PΔE in Appendix B.

Analysis of resonance conditions

We analyse possible resonant terms for the summations in Eq. (A6). For the last summation, with $m = k + p + q$, we identify three distinct resonance scenarios:

$$\omega_m = \omega_p + \omega_q + \omega_k, \tag{Case 1}$$

$$\omega_m = \omega_p + \omega_q - \omega_k, \tag{Case 2}$$

$$\omega_m = \omega_k - \omega_p - \omega_q. \tag{Case 3}$$

Next, we consider the second summation in Eq. (A6), where $m = k - p - q$. Indices can be rearranges as $k = m + p + q$, leading to resonance scenarios that are equivalent to (Case 1)-(Case 3). Specifically:

$$\begin{aligned} &\omega_m = \omega_p + \omega_q + \omega_k \\ \Leftrightarrow &\omega_k = \omega_m - \omega_p - \omega_q \equiv (Case3), \\ &\omega_m = \omega_p + \omega_q - \omega_k \\ \Leftrightarrow &\omega_k = \omega_p + \omega_q - \omega_m \equiv (Case2), \\ &\omega_m = \omega_k - \omega_p - \omega_q \\ \Leftrightarrow &\omega_k = \omega_m + \omega_p + \omega_q \equiv (Case1). \end{aligned}$$

For the first summation in Eq. (A6), where $m = p+q-k$, we obtain three additional resonance scenarios:

$$\omega_m = \omega_p + \omega_q + \omega_k, \tag{Case 4}$$

$$\omega_m = \omega_p - \omega_q + \omega_k, \tag{Case 5}$$

$$\omega_m = \omega_p + \omega_q - \omega_k. \tag{Case 6}$$

We now investigate whether any of the six resonance conditions above hold under the assumptions (i.e. (Cond-1)-(Cond-5)) on the natural frequency.

Proposition 1 *Under the frequency conditions (Cond-1)–(Cond-5), none of the resonance conditions (Case 1)–(Case 4) can occur.*

Proof **Case 1:** Suppose $\omega_m = \omega_p+\omega_q+\omega_k$. Then $\omega_{p+q+k} = \omega_k + \omega_p + \omega_q$. However, by the sub-additivity condition (Cond-4), we have:

$$\omega_{p+q+k} < \omega_p + \omega_q + \omega_k, \tag{A8}$$

which is a contradiction. Hence, Case 1 cannot occur.
Case 2: Suppose $\omega_m = \omega_p + \omega_q - \omega_k$. Using (Cond-1), we get

$$\omega_{p+q+k} = \omega_p + \omega_q - \omega_k < \omega_p + \omega_q. \tag{A9}$$

Using (Cond-5), we write:

$$\begin{aligned} \pi(p+q+k) &< \omega_{p+q+k} && \text{(A10)}\\ &< \omega_p + \omega_q && \text{(A11)}\\ &< \pi(p+\tfrac{1}{2}) + \pi(q+\tfrac{1}{2}). && \text{(A12)} \end{aligned}$$

Subtracting $\pi(p+q)$ from both sides yields

$$\pi k < \omega_p - \pi p + \omega_q - \pi q < \frac{\pi}{2} + \frac{\pi}{2} = \pi. \tag{A13}$$

This implies $k < 1$, contradicting the assumption that $k \in \mathbb{N}^+$. Thus, Case 2 cannot occur.
Case 3: Suppose $\omega_m = \omega_k - \omega_p - \omega_q$. Then,

$$\omega_k = \omega_{p+q+k} + \omega_p + \omega_q > \omega_k + \omega_p + \omega_q > \omega_k \tag{A14}$$

again a contradiction. Therefore, Case 3 cannot occur.
Case 4: Assume $\omega_m = \omega_k + \omega_p + \omega_q$ with $m = p+q-k$. Then, it follows from (Cond-1) and (Case 4), that

$$\omega_k + \omega_p + \omega_q = \omega_{p+q-k} < \omega_{p+q} < \omega_p + \omega_q + \omega_k, \tag{A15}$$

which is a contradiction. So, Case 4 cannot occur. □

Proposition 2 *Under the frequency conditions (Cond-1)–(Cond-5), none of the resonance conditions (Case 5)–(Case 6) can occur, except in the degenerate cases where the indices satisfy $m = p$, $k = q$ or $m = q$, $k = p$.*

Proof **Case 5:** Suppose $\omega_m = \omega_k + \omega_p - \omega_q$ with $m = p+q-k$, implying $m+k = p+q$.
We consider three scenarios:

- If $m > p$ and $k < q$, then from (Cond-2),

$$\omega_m + \omega_q > \omega_p + \omega_k, \tag{A16}$$

a contradiction.

- If $m < p$ and $k > q$, then again, from (Cond-2),

$$\omega_m + \omega_q < \omega_p + \omega_k, \tag{A17}$$

again a contradiction.
- If $m = p$ and $k = q$, then clearly

$$\omega_m + \omega_q = \omega_k + \omega_p, \tag{A18}$$

thus Case 5 is satisfied.

Case 6: Suppose $\omega_m = \omega_p + \omega_q - \omega_k$ with $m = p+q-k$. Let $c := p+q \in \mathbb{N}^+$, and we want to prove the inequality

$$\omega_{c-i} + \omega_i > \omega_{c-i-1} + \omega_{i+1} \tag{A19}$$

for some $i \in \mathbb{N}$ with $c - i > i$. Using convexity (Cond-3), we write

$$\begin{aligned} &\sum_{j=0}^{c-2(i+1)} \Delta^2 \omega_{i+j} = \Delta^2 \sum_{j=0}^{c-2(i+1)} E^j \omega_i \\ &= (E-I)^2 \sum_{j=0}^{c-2(i+1)} E^j \omega_i \\ &= (E-I)\big(E^{c-2i-1} - I\big)\omega_i \\ &= \big(E^{c-2i} - E - E^{c-2i-1} + I\big)\omega_i > 0 \\ &\Leftrightarrow (E^{c-2i} + I)\omega_i > (E^{c-2i-1} - E)\omega_i \\ &\Leftrightarrow \omega_{c-i} + \omega_i > \omega_{c-i-1} + \omega_{i+1}. \end{aligned} \tag{A20}$$

Following induction, it is evident that for $m > k$ and $p > q$ (without loss of generality), we obtain:

$$\omega_m + \omega_k > \omega_p + \omega_q, \tag{A21}$$

which contradicts the resonance condition (Case 6). Similarly, for $m < k$ and $p < q$, the inequality reverses direction and again leads to a contradiction.

Thus, (Case 6) cannot occur except for $m = p$, $k = q$, or $m = q$, $k = p$. □

Following Proposition 1 and 2, Eq. (A5) reduces to

$$\begin{aligned} &\varepsilon\left(\frac{\Delta_{n_0}^2}{\phi_{t,m}} + \lambda_m E_{n_0}\right) V_{1m} \\ &= -\frac{\Delta_{n_1} H_m}{\phi_{t,m}} + \varepsilon \frac{H_m}{\psi_{t,m}} \\ &\quad - \varepsilon \frac{1}{8\psi_{t,m}^3}\left(H_m^3 + 2\sum_{k\neq m}^{\infty} H_k^2 H_m\right) + \text{n.r.t.} \end{aligned} \tag{A22}$$

Appendix B Verification of the frequency conditions

We verify that natural frequencies defined in (118)-(119) satisfy (Cond-1)-(Cond-5).

B.1 PDE frequencies

For $\omega_k = \sqrt{1+\pi^2 k^2}$ from (119) all five conditions trivially satisfied: ω_k is positive, increasing, convex, sub-additive and satisfying $\pi k < \omega_k < \pi(k+\frac{1}{2})$; the reader can verify these properties directly.

B.2 Standard PΔE frequencies

We now verify (Cond-1)-(Cond-5) for the discrete natural frequency in (118). For fixed Δt and Δx, we define the continuous extensions (from $\mathbb{R}^+$ to $\mathbb{R}^+$)

$$\begin{aligned}\lambda(k) &:= 1 + \tfrac{4}{(\Delta x)^2}\sin^2(\tfrac{k\pi\Delta x}{2}),\\ \omega(k) &:= \tfrac{1}{\Delta t}\arcsin\left(\sqrt{(\Delta t)^2\lambda(k) - \tfrac{(\Delta t)^4\lambda(k)^2}{4}}\right).\end{aligned} \tag{B23}$$

To ensure real and unique natural frequencies, we consider $0 < \phi_t\lambda(k) < 4$ and $0 < k < \frac{1}{\Delta x}$, within which $\lambda(k)$ is strictly increasing. ***Condition-1***

From (B23), $\omega(k)$ is real and positive whenever $0 < \lambda_k < \frac{4}{\phi_t}$, which gives

$$|\sin(\tfrac{k\pi\Delta x}{2})| < \tfrac{\Delta x}{\Delta t}\sqrt{1-\tfrac{(\Delta t)^2}{4}}. \tag{B24}$$

If the right-hand side exceeds one, the inequality is automatically satisfied for all k. This occurs when

$$\Delta t < \frac{\Delta x}{\sqrt{1+\frac{(\Delta x)^2}{4}}}. \tag{B25}$$

Otherwise, when $\frac{\Delta x}{\Delta t}\sqrt{1-\frac{(\Delta t)^2}{4}} < 1$ and $\sin(\frac{k\pi\Delta x}{2})$ is monotone (i.e. for $k\Delta x < 1$), this yields the bound

$$k < \tfrac{2}{\pi\Delta x}\arcsin(\tfrac{\Delta x}{\Delta t}\sqrt{1-\tfrac{(\Delta t)^2}{4}}). \tag{B26}$$

Hence, (Cond-1) is satisfied for k in this range.

For small steps, (B26) can be approximated as follows: for $\Delta x = \Delta t \ll 1$:

$$k_{\max} \simeq \frac{1}{\Delta t} - \frac{1}{\pi} + \mathcal{O}((\Delta t)^2), \tag{B27}$$

and for a more general case $\Delta x = \Delta t + c(\Delta t)^2 + \mathcal{O}((\Delta t)^2)$ with $\Delta t \ll 1$ and $c = \mathcal{O}(1)$:

$$k_{\max} \simeq \tfrac{1}{\Delta t} - \tfrac{2\sqrt{-2c}}{\sqrt{\Delta t}} - c + \mathcal{O}\left(\sqrt{\Delta t}\right), \tag{B28}$$

for $c < 0$. These bounds specify the highest spatial mode for which $\omega(k)$ satisfies (Cond-1).

Condition-2

To ensure $\Delta\omega_k > 0$, it is sufficient to show that $\frac{d\omega(k)}{dk} > 0$. From (B23), define

$$f(k) := \phi_t\lambda(k) - \frac{\phi_t^2\lambda^2(k)}{4}, \tag{B29}$$

which satisfies $f(k) > 0$ for $0 < \lambda(k) < \frac{4}{\phi_t}$. Since $f(k) = \sin^2(\omega(k)\Delta t)$, it follows that $1 - f(k) = \cos^2(\omega(k)\Delta t) > 0$, hence $\sqrt{1-f(k)} > 0$. Differentiating (B23) gives

$$\omega'(k) = \frac{f'(k)}{2\Delta t\sqrt{f(k)}\sqrt{1-f(k)}}. \tag{B30}$$

So $\omega'(k)$ whenever $f'(k) > 0$.

Because

$$f'(k) = \phi_t\lambda'(k)(1 - \tfrac{\phi_t\lambda(k)}{2}), \tag{B31}$$

$f'(k)$ requires both $\lambda'(k)$ and $1 - \frac{\phi_t\lambda(k)}{2}$ being positive or negative. The later case $\lambda'(k) < 0$ excludes the modal interval where $\omega_k > 0$, hence only the first case is relevant for the present analysis. $\lambda'(k) > 0$ holds for $0 < k < \frac{1}{\Delta x}$, where $\lambda'(k) = \frac{2\pi k}{\Delta x}\sin(\pi k\Delta x)$.

The second condition, $1 - \frac{\phi_t\lambda(k)}{2} > 0$, yields

$$k < \tfrac{2}{\pi\Delta x}\arcsin(\tfrac{\Delta x}{2\Delta t}\sqrt{2-(\Delta t)^2}). \tag{B32}$$

For small steps with $\Delta x = \Delta t \ll 1$, this can be approximated by

$$k_{\max} \simeq \frac{1}{2\Delta t} - \frac{\Delta t}{2\pi} + \mathcal{O}((\Delta t)^5), \tag{B33}$$

and for a more general case $\Delta x = \Delta t + c(\Delta t)^2$ with $\Delta t \ll 1$, we obtain

$$\begin{aligned}k_{\max} \simeq &\tfrac{1}{2\Delta t} + \tfrac{2c}{\pi}(1-\tfrac{\pi}{4}) + \tfrac{1}{2\pi}((\pi-2)c^2 - 1)\Delta t\\ &+ \mathcal{O}((\Delta t)^2).\end{aligned} \tag{B34}$$

Thus combining (Cond-1) and (Cond-2), the lowest upper bound corresponds to $\phi_t\lambda < 2$.

Condition-3

Analogous to the monotonicity argument in Condition-2, discrete convexity ($\Delta^2\omega_k > 0$) follows from the continuous convexity condition $\omega''(k) > 0$. Differentiating (B30) once again with respect to k, we obtain

$$\omega''(k) = \frac{2f''f(1-f)-(f')^2(1-2f)}{4\Delta t f^{\frac{3}{2}}(1-f)^{\frac{3}{2}}} > 0, \tag{B35}$$

where the denominator is positive, (B35) is positive when numerator is positive, i.e.

$$2f''f(1-f) - (f')^2(1-2f) > 0. \tag{B36}$$

Substituting $f(k) = \phi_t\lambda(k) - \frac{\phi_t^2\lambda^2(k)}{4}$ gives

$$\frac{\phi_t}{16}(\phi_t\lambda - 2)^3((2-\phi_t\lambda)(\lambda')^2 + \lambda(\phi\lambda - 4)\lambda'') > 0. \tag{B37}$$

As shown in Condition-2, we have $\phi_t\lambda < 2$. To determine the upper bound for k, we shall study the interval for which

$$(2-\phi_t\lambda)(\lambda')^2 + \lambda(\phi\lambda - 4)\lambda'' < 0. \tag{B38}$$

Considering the case where $\Delta x = \Delta t \ll 1$, this inequality simplifies to

$$\begin{aligned}&(2-\phi_t\lambda)(\lambda')^2 + \lambda(\phi\lambda - 4)\lambda'' \\ &= -2\pi^2(3 - (\Delta x)^2\cos(k\pi\Delta x) + \cos(2k\pi\Delta x)) < 0\end{aligned} \tag{B39}$$

showing that $\omega''(k) > 0$ for all $k < \frac{1}{\Delta x}$. Thus the same upper bound obtained in Condition-2 $\phi_t\lambda(k) < 2$ also guarantees convexity.

Further assuming, for more general case, $\Delta x = \Delta t + c(\Delta t)^2$ with $\Delta t \ll 1$ yields

$$\begin{aligned}&(2-\phi_t\lambda)(\lambda')^2 + \lambda(\phi\lambda - 4)\lambda'' \\ &= -2\pi^2\Big[\frac{32c}{\Delta x}\sin^4(\tfrac{k\pi\Delta x}{2}) - 8c^2\cos(k\pi\Delta x) \\ &\quad + (1+2c^2)(3+\cos(2k\pi\Delta x)) \\ &\quad + 16c(\Delta x)\sin^4(\tfrac{k\pi\Delta x}{2}) + \mathcal{O}((\Delta x)^2)\Big] < 0.\end{aligned} \tag{B40}$$

This similarly holds for all modes when $\Delta t \ll 1$. Therefore, for $\Delta x = \Delta t + c(\Delta t)^2$, we again have $1 - \frac{\phi_t\lambda(k)}{2} > 0$ as the condition on mode number k.

Condition-5

We now determine the interval of mode number k for which (Cond-5) holds, i.e. $\pi k < \omega_k < \pi(k+\frac{1}{2})$. To establish the upper bound, we aim show that $\omega(0) < \frac{\pi}{2}$ and, for a given interval in k, that $\omega'(k) \le \pi$. Using the fundamental theorem of calculus, we write

$$\omega(k) < \omega(0) + \int_0^k \omega'(s)ds \le \pi(k+\tfrac{1}{2}). \tag{B41}$$

From (B23),

$$\omega(0) = \tfrac{1}{\Delta t}\arcsin(\sqrt{(\Delta t)^2 - \tfrac{(\Delta t)^4}{4}}) < \frac{\pi}{2} \tag{B42}$$

where $(\Delta t)^2 - \frac{(\Delta t)^4}{4} < \sin^2(\frac{\pi\Delta t}{2})$ for $\Delta t \ll 1$.
For $\omega'(k) \le \pi$, using (B29)-(B31), we have

$$\lambda'(k) \le 2\pi\sqrt{\lambda(k) - \tfrac{(\Delta t)^2\lambda^2(k)}{4}}. \tag{B43}$$

Substituting the expressions of $\lambda(k)$ and $\lambda'(k)$ and squaring of both sides, then multiplying each term by $(\Delta x)^2$ yields

$$\begin{aligned}0 \le &(\Delta x)^2(1 - \tfrac{(\Delta t)^2}{4}) + 2\sin^2(\tfrac{k\pi\Delta x}{2})\Big[1 - (\Delta t)^2 \\ &+ (1 - \tfrac{2(\Delta t)^2}{(\Delta x)^2})\sin^2(\tfrac{k\pi\Delta x}{2})\Big].\end{aligned} \tag{B44}$$

This expression can be written as a polynomial in $S = \sin^2(\frac{k\pi\Delta x}{2})$. Dividing (B44) by 2 yields

$$P(S) := a_2S^2 + a_1S + a_0 \ge 0, \tag{B45}$$

where

$$\begin{aligned}a_0 &:= \tfrac{\Delta x^2}{2}(1 - \tfrac{\Delta t^2}{4}), \\ a_1 &:= 1 - \Delta t^2, \\ a_2 &:= 1 - 2\tfrac{\Delta t^2}{\Delta x^2}.\end{aligned} \tag{B46}$$

Note that $S \in [0,1]$, and since $0 < \Delta t, \Delta x \ll 1$ we have $a_0, a_1 > 0$. Hence, there are two distinct scenarios for this polynomial: $a_2 \ge 0$ and $a_2 < 0$.

If $a_2 \ge 0$ (equivalently $\Delta t \le \Delta x/\sqrt{2}$), then $P(S) \ge a_0 > 0$ for all $S \in [0,1]$, and thus inequality (B44) is satisfied.

If $a_2 < 0$, $P(S)$ is concave, so $P(S) \ge 0$ holds for $S \in [S_-, S_+]$, where $S_\pm$ are the (real) roots. Writing $\tilde{a}_2 = -a_2 > 0$, we obtain

$$S_\pm = \tfrac{a_1}{2\tilde{a}_2} \mp \tfrac{\sqrt{a_1^2 + 4a_0\tilde{a}_2}}{2\tilde{a}_2}. \tag{B47}$$

Since $S_- < 0 < S_+$, it follows that $P(S) \ge 0$ for $S \in [0, \min\{1, S_+\}]$. We obtain $S_+ > 1$ when

$$\tfrac{2\Delta x}{\sqrt{\Delta x^2 + 4}} > \Delta t > \tfrac{\Delta x}{\sqrt{2}}, \tag{B48}$$

meaning that $[0,1] \cap [S_-, S_+] = [0,1]$, and therefore(B44) is directly satisfied. On the other hand, we obtain $S_+ < 1$ when

$$\frac{2\Delta x}{\sqrt{\Delta x^2+4}} < \Delta t, \tag{B49}$$

so that $[0,1] \cap [S_-, S_+] = [0, S_+]$.For the upper bound we require $S < S_+$, which is equivalent to

$$\sin^2(\tfrac{k\pi\Delta x}{2}) < \tfrac{1}{2\tilde{a}_2}\left(a_1 + \sqrt{a_1^2 + 4a_0\tilde{a}_2}\right), \tag{B50}$$

which leads to

$$k < \tfrac{2}{\pi\Delta x}\arcsin\left(\sqrt{\tfrac{1}{2\tilde{a}_2}(a_1 + \sqrt{a_1^2 + 4a_0\tilde{a}_2})}\right). \tag{B51}$$

For the special case $\Delta x = \Delta t \ll 1$, this simplifies to

$$k_{\max} \simeq \tfrac{1}{\Delta t} - \tfrac{2}{\pi} + \mathcal{O}((\Delta t)^2). \tag{B52}$$

For a more general case $\Delta x = \Delta t + c(\Delta t)^2$ with $\Delta t \ll 1$, we obtain

$$\begin{aligned} k_{\max} \simeq & \tfrac{1}{\Delta t} - \tfrac{4\sqrt{-c}}{\pi\sqrt{\Delta t}} - c + \tfrac{3+20^2}{12c\pi}\sqrt{-c\Delta t} \\ & + \mathcal{O}(\Delta t), \end{aligned} \tag{B53}$$

where $c < 0$.

We now obtain the modal interval for k where $\pi k < \omega_k$. From (B23),

$$\pi k\Delta t < \arcsin\left(\sqrt{\phi_t\lambda(k) - \frac{\phi_t^2\lambda(k)^2}{4}}\right) \tag{B54}$$

which leads to

$$\sin^2(\pi k\Delta t) < \phi_t\lambda(k) - \frac{\phi_t^2\lambda(k)^2}{4}. \tag{B55}$$

Equivalently,

$$\phi_t^2\lambda(k)^2 - 4\phi_t\lambda(k) + 4\sin^2(\pi k\Delta t) < 0, \tag{B56}$$

a parabola in λ, with discriminant $16\cos^2(\pi k\Delta t) \geq 0$ and roots

$$\lambda_\pm = \tfrac{2}{(\Delta t)^2}(1 \pm \cos(k\pi\Delta t)). \tag{B57}$$

Hence, the admissible range of mode numbers k (i.e. those satisfying $\pi k < \omega_k$) is determined by the inequality

$$\tfrac{4}{(\Delta t)^2}\sin^2(\tfrac{\pi k\Delta t}{2}) < \lambda(k) < \tfrac{4}{(\Delta t)^2}\cos^2(\tfrac{\pi k\Delta t}{2}). \tag{B58}$$

With $\lambda(k) = 1 + \frac{4}{(\Delta x)^2}\sin^2(\frac{k\pi\Delta x}{2})$, the lower inequality is trivial for $\Delta x = \Delta t \ll 1$, so the range of validity in mode number k is determined by the upper inequality, which gives

$$1 + \tfrac{4}{(\Delta t)^2}\sin^2(\tfrac{k\pi\Delta t}{2}) < \tfrac{4}{(\Delta t)^2}\cos^2(\tfrac{\pi k\Delta t}{2}) \tag{B59}$$

which leads to

$$1 < \tfrac{4}{(\Delta t)^2}\cos(\pi k\Delta t), \tag{B60}$$

which means

$$k_{\max} \simeq \tfrac{1}{2\Delta t} - \tfrac{\Delta t}{4\pi} + \mathcal{O}((\Delta t)^5). \tag{B61}$$

For $\Delta x = \Delta t + c(\Delta t)^2$ with $\Delta t \ll 1$: similarly, the lower bound is trivial. For the upper bund we get

$$\cos(k\pi\Delta t) + \frac{\cos(\frac{k\pi\Delta t}{1+c\Delta t}) - 1}{(1+c\Delta t)^2} + 1 - \tfrac{(\Delta t)^2}{2} > 0. \tag{B62}$$

Following the bound obtained in (B61), we expand given expressions near $k = \frac{1}{2\Delta t}$, we obtain

$$\begin{aligned} k_{\max} \simeq & \tfrac{1}{2\Delta t} + c(\tfrac{1}{\pi} - \tfrac{1}{4}) - \tfrac{2+c^2(8-3\pi)}{8\pi}\Delta t \\ & + \mathcal{O}((\Delta t)^2). \end{aligned} \tag{B63}$$

Condition-4

Finally, we verify the strict sub-additivity condition,

$$\omega_{a+b} < \omega_a + \omega_b. \tag{B64}$$

To prove this, we use the known fact that "$\frac{\omega_k}{k}$ decreasing implies sub-additivity". Using the continuous arguments, we have

$$\begin{aligned} \tfrac{d}{dk}(\tfrac{\omega(k)}{k}) = \tfrac{\omega'(k)k - \omega(k)}{k^2} < 0 \\ \Leftrightarrow \omega'(k)k < \omega(k). \end{aligned} \tag{B65}$$

We have proved for (Cond-5) that $\omega'(k) \leq \pi$ and $\omega(k) > \pi k$ for $k \lesssim \frac{1}{2\Delta t}$. Hence we can write

$$k\omega'(k) \leq \pi k < \omega(k), \tag{B66}$$

which proves that $\omega(k)$ (and thus ω_k) is sub-additive.

Thus, we have shown all scenarios for the mode number that satisfy the conditions (Cond-1)-(Cond-5). For special scenarios, where $\Delta x \simeq \Delta t \ll 1$, the approximate bound on the total number of modes is obtained as $k \lesssim \frac{1}{2\Delta x}$.

Acknowledgements The authors thank the anonymous reviewers for their constructive comments, which helped improve the manuscript.

Author Contributions E.K. contributed to conceptualisation, methodology, investigation, formal analysis, visualisation, and writing - original draft. W.T.vH. contributed to conceptualisation, methodology, supervision, validation, and writing - review and editing. All authors have read and approved the final version of the manuscript.

Funding This research received no external funding.

Data Availability No datasets were generated or analysed during the current study.

Declarations

Conflict of interest The authors declare no Conflict of interest.

References

1. Holmes, M.H.: Introduction to Perturbation Methods. Texts in Applied Mathematics, vol. 20. Springer, New York, NY (2013). https://doi.org/10.1007/978-1-4614-5477-9
2. Kevorkian, J., Cole, J.D.: Multiple Scale and Singular Perturbation Methods. Applied Mathematical Sciences, vol. 114. Springer, New York, NY (1996). https://doi.org/10.1007/978-1-4612-3968-0
3. Nayfeh, A.H.: Perturbation Methods, 1st edn. Wiley-VCH Verlag GmbH & Co. KGaA, Weinheim (2000). https://doi.org/10.1002/9783527617609
4. Verhulst, F.: Methods and Applications of Singular Perturbations. Texts in Applied Mathematics, vol. 50. Springer, New York, NY (2005). https://doi.org/10.1007/0-387-28313-7
5. Sanders, J.A., Verhulst, F., Murdock, J.: Averaging Methods in Nonlinear Dynamical Systems. Applied Mathematical Sciences, vol. 59. Springer, New York, NY (2007). https://doi.org/10.1007/978-0-387-48918-6
6. Binatari, N., Van Horssen, W.T., Verstraten, P., Adi-Kusumo, F., Aryati, L.: On the multiple time-scales perturbation method for differential-delay equations. Nonlinear Dyn. **112**(10), 8431–8451 (2024). https://doi.org/10.1007/s11071-024-09485-z
7. Torng, H.C.: Second-order non-linear difference equations containing small parameters. J. Franklin Inst. **269**(2), 97–104 (1960). https://doi.org/10.1016/0016-0032(60)90049-1
8. Huston, R.L.: Krylov-Bogoljubov Method for Difference Equations. SIAM J. Appl. Math. **19**(2), 334–339 (1970). https://doi.org/10.1137/0119031
9. Hoppensteadt, F.C., Miranker, W.L.: Multitime methods for systems of difference equations. Stud. Appl. Math. **56**(3), 273–289 (1977). https://doi.org/10.1002/sapm1977563273
10. Subramanian, R., Krishnan, A.: Non-linear discrete time systems analysis by multiple time perturbation techniques. J. Sound Vib. **63**(3), 325–335 (1979). https://doi.org/10.1016/0022-460X(79)90677-1
11. Van Horssen, W.T., Ter Brake, M.C.: On the multiple scales perturbation method for difference equations. Nonlinear Dyn. **55**(4), 401–418 (2009). https://doi.org/10.1007/s11071-008-9373-z
12. Hall, C.L., Lustri, C.J.: Multiple scales and matched asymptotic expansions for the discrete logistic equation. Nonlinear Dyn. **85**(2), 1345–1362 (2016). https://doi.org/10.1007/s11071-016-2764-7

13. Liu, C.S.: The renormalization method from continuous to discrete dynamical systems: asymptotic solutions, reductions and invariant manifolds. Nonlinear Dyn. **94**(2), 873–888 (2018). https://doi.org/10.1007/s11071-018-4399-3
14. Newell, A.C.: Finite amplitude instabilities of partial difference equations. SIAM J. Appl. Math. **33**(1), 133–160 (1977). https://doi.org/10.1137/0133010
15. Hyatt, B.A., Lecoanet, D., Anders, E.H., Burns, K.J.: Multiple scales analysis of a nonlinear timestepping instability in simulations of solitons. J. Comput. Phys. **531**, 113923 (2025). https://doi.org/10.1016/j.jcp.2025.113923
16. Mickens, R.E.: Periodic solutions of second-order nonlinear difference equations containing a small parameter-IV. Multi-discrete time method. J. Franklin Inst. **324**(2), 263–271 (1987). https://doi.org/10.1016/0016-0032(87)90065-2
17. Mickens, R.E.: Calculation of order ε dynamics for an NSFD discretization of a cube-root damped oscillator. J. Differ. Equ. Appl. **20**(5–6), 826–836 (2014). https://doi.org/10.1080/10236198.2013.822866
18. Marathe, A., Chatterjee, A.: Wave attenuation in nonlinear periodic structures using harmonic balance and multiple scales. J. Sound Vib. **289**(4–5), 871–888 (2006). https://doi.org/10.1016/j.jsv.2005.02.047
19. Mickens, R.E.: Nonstandard Finite Difference Schemes: Methodology and Applications. World Scientific, New Jersey London Singapore Beijing Shanghai Hong Kong Taipei Chennai Tokyo (2021)
20. Anguelov, R., Lubuma, J.M.S.: Contributions to the mathematics of the nonstandard finite difference method and applications. Numer. Methods Partial **17**(5), 518–543 (2001). https://doi.org/10.1002/num.1025
21. Mickens, R.E., Jordan, P.M.: A positivity-preserving nonstandard finite difference scheme for the damped wave equation. Numer. Methods Partial **20**(5), 639–649 (2004). https://doi.org/10.1002/num.20003
22. Chapwanya, M., Lubuma, J.M.S., Mickens, R.E.: Nonstandard finite difference schemes for Michaelis-Menten type reaction-diffusion equations. Numer. Methods Partial **29**(1), 337–360 (2013). https://doi.org/10.1002/num.21733
23. Aderogba, A.A., Chapwanya, M.: An explicit nonstandard finite difference scheme for the Allen-Cahn equation. J. Differ. Equ. Appl. **21**(10), 875–886 (2015). https://doi.org/10.1080/10236198.2015.1055737
24. De Waal, G.N., Appadu, A.R., Pretorius, C.J.: Some standard and nonstandard finite difference schemes for a reaction-diffusion-chemotaxis model. Open Phys. **21**(1), 20220231 (2023). https://doi.org/10.1515/phys-2022-0231
25. Keller, J.B., Kogelman, S.: Asymptotic solutions of initial value problems for nonlinear partial differential equations. SIAM J. Appl. Math. **18**(4), 748–758 (1970). https://doi.org/10.1137/0118067